
Radiation Dose Estimates and Hazard Evaluations for Inhaled Airborne Radionuclides

Annual Progress Report
July 1981 - June 1982

Prepared by J. A. Mewhinney

Inhalation Toxicology Research Institute
Lovelace Biomedical and Environmental Research Institute

Prepared for
U.S. Nuclear Regulatory
Commission

NOTICE

This report was prepared as an account of work sponsored by an agency of the United States Government. Neither the United States Government nor any agency thereof, or any of their employees, makes any warranty, expressed or implied, or assumes any legal liability of responsibility for any third party's use, or the results of such use, of any information, apparatus, product or process disclosed in this report, or represents that its use by such third party would not infringe privately owned rights.

Availability of Reference Materials Cited in NRC Publications

Most documents cited in NRC publications will be available from one of the following sources:

1. The NRC Public Document Room, 1717 H Street, N.W.
Washington, DC 20555
2. The NRC/GPO Sales Program, U.S. Nuclear Regulatory Commission,
Washington, DC 20555
3. The National Technical Information Service, Springfield, VA 22161

Although the listing that follows represents the majority of documents cited in NRC publications, it is not intended to be exhaustive.

Referenced documents available for inspection and copying for a fee from the NRC Public Document Room include NRC correspondence and internal NRC memoranda; NRC Office of Inspection and Enforcement bulletins, circulars, information notices, inspection and investigation notices; Licensee Event Reports; vendor reports and correspondence; Commission papers; and applicant and licensee documents and correspondence.

The following documents in the NUREG series are available for purchase from the NRC/GPO Sales Program: formal NRC staff and contractor reports, NRC-sponsored conference proceedings, and NRC booklets and brochures. Also available are Regulatory Guides, NRC regulations in the *Code of Federal Regulations*, and *Nuclear Regulatory Commission Issuances*.

Documents available from the National Technical Information Service include NUREG series reports and technical reports prepared by other federal agencies and reports prepared by the Atomic Energy Commission, forerunner agency to the Nuclear Regulatory Commission.

Documents available from public and special technical libraries include all open literature items, such as books, journal and periodical articles, and transactions. *Federal Register* notices, federal and state legislation, and congressional reports can usually be obtained from these libraries.

Documents such as theses, dissertations, foreign reports and translations, and non-NRC conference proceedings are available for purchase from the organization sponsoring the publication cited.

Single copies of NRC draft reports are available free upon written request to the Division of Technical Information and Document Control, U.S. Nuclear Regulatory Commission, Washington, DC 20555.

Copies of industry codes and standards used in a substantive manner in the NRC regulatory process are maintained at the NRC Library, 7920 Norfolk Avenue, Bethesda, Maryland, and are available there for reference use by the public. Codes and standards are usually copyrighted and may be purchased from the originating organization or, if they are American National Standards, from the American National Standards Institute, 1430 Broadway, New York, NY 10018.

Radiation Dose Estimates and Hazard Evaluations for Inhaled Airborne Radionuclides

Annual Progress Report
July 1981 - June 1982

Manuscript Completed: February 1983
Date Published: June 1983

Prepared by
J. A. Mewhinney

Inhalation Toxicology Research Institute
Lovelace Biomedical and Environmental Research Institute
P. O. Box 5890
Albuquerque, NM 87185

Prepared for
Division of Health, Siting and Waste Management
Office of Nuclear Regulatory Research
U.S. Nuclear Regulatory Commission
Washington, D.C. 20555
NRC FIN A1031

PREVIOUS DOCUMENTS IN SERIES

1. Radiation Exposure and Risk Estimates for Inhaled Airborne Radioactive Pollutants Including Hot Particles, Annual Progress Report, 1976-1977, NUREG/CR-0010, 1978.
2. Radiation Dose Estimates and Hazard Evaluations for Inhaled Airborne Radionuclides, Annual Progress Report, 1977-1978, NUREG/CR-0673, 1979.
3. Radiation Dose Estimates and Hazard Evaluations for Inhaled Airborne Radionuclides, Annual Progress Report, 1978-1979, NUREG/CR-1458, 1980.
4. Comparison of Physical Chemical Properties of Powders and Respirable Aerosols of Industrial Mixed Uranium and Plutonium Oxide Fuels, NUREG/CR-1736, 1980.
5. In Vitro Dissolution of Respirable Aerosols of Industrial Uranium and Plutonium Mixed Oxide Nuclear Fuels, NUREG/CR-2171, 1981.
6. Particle Analysis of Mixed-Oxide Nuclear Fuel Materials by Energy Dispersive X-Ray Fluorescence, NUREG/CR-1871, 1981.
7. Radiation Dose Estimates and Hazard Evaluations for Inhaled Airborne Radionuclides, Annual Progress Report, 1979-1980, NUREG/CR-2246, 1981.
8. Radiation Dose Estimates and Hazard Evaluations for Inhaled Airborne Radionuclides, Annual Progress Report, 1980-1981, NUREG/CR-2512, 1982.

ABSTRACT

The objective of this project is to conduct confirmatory research on aerosol characteristics and the resulting radiation dose distribution in animals following inhalation and to provide prediction of health consequences in humans due to airborne radioactivity which might be released in normal operations or under accident conditions during production of nuclear fuel composed of mixed oxides of U and Pu. Four research reports summarize the results of specific areas of research conducted. The first paper, presented in three parts, details the development of a new method for determination of the specific surface area of very small samples of particles of hazardous materials, the comparison of this method with two other methods of specific surface area determination and the application of the new method to measurement of the specific surface area of mixed oxide or pure PuO_2 particles used in the animal inhalation studies in this project.

The second paper details the extension of the biomathematical model previously used to describe the retention, distribution and excretion of Pu from these mixed oxide aerosols to include a description of the Am and U components of the mixed oxides in dogs, monkeys and rats. This extended model uses to the new information developed from specific surface area measurement of the particulates. The third paper summarizes the biological responses observed in the three radiation dose pattern studies in which dogs, monkeys and rats received inhalation exposures to either 750°C heat-treated $\text{UO}_2 + \text{PuO}_2$, 1750°C heat-treated $(\text{U,Pu})\text{O}_2$ or 850°C heat-treated "pure" PuO_2 . The dose-response studies in which rats were exposed to $(\text{U, Pu})\text{O}_2$ or "pure" PuO_2 are the subject of the fourth paper in this report. This paper updates earlier reports and summarizes the status of animals in these studies through approximately 650 days after inhalation.

TABLE OF CONTENTS

	<u>Page</u>
ABSTRACT.....	iii
LIST OF FIGURES.....	vi
LIST OF TABLES.....	viii
ACKNOWLEDGMENTS.....	ix
EXECUTIVE SUMMARY.....	1
1. SURFACE AREA MEASUREMENTS	
Part A. Measurement of Specific Area of Small Powder Samples Using ⁸⁵ Kr as Adsorbate.....	3
Part B. A Comparison of Three Methods of Determining Specific Surface Area and a Comparison of Three Materials for Surface Area Standards.....	11
Part C. Specific Surface Area Determinations of Mixed U and Pu Oxide Particulates.....	16
2. MODELS OF RETENTION, DISTRIBUTION AND EXCRETION OF Pu, Am and U BY BEAGLE DOGS, CYNOMOLGUS MONKEYS AND FISCHER-344 RATS FOLLOWING INHALATION OF INDUSTRIAL AEROSOLS.....	21
3. BIOLOGICAL EFFECTS IN RATS, DOGS AND MONKEYS AFTER INHALATION OF INDUSTRIAL MIXED OXIDES OR PuO ₂	33
4. DOSE-RESPONSE STUDIES IN FISCHER-244 RATS.....	41
APPENDIX A — STATUS OF INHALATION STUDIES.....	51

LIST OF FIGURES

Page

Figure 1-1.	Schematic diagram of ^{85}Kr adsorption apparatus. A sample and a standard powder of known specific surface area are attached to the vacuum manifold. The system is evacuated to 10^{-5} Torr and the sample and standard powder heated to 250°C for ~ 16 hours. Krypton-85 is then admitted from the reservoir and the sample and standard powders adsorb ^{85}Kr when cooled in liquid nitrogen. Taps to sample and standard powder cells are closed, the cells removed to a counting station to quantify the ^{85}Kr adsorbed.....	4
Figure 1-2.	Sample and standard powder cells used for ^{85}Kr adsorption; a) type I cell, b) type II cell and c) type III cell. In type II and III cells, the amount of glass cooled sufficiently to adsorb ^{85}Kr is nearly independent of the liquid nitrogen level provided it is between points A and B.....	5
Figure 1-3.	Variation of specific surface area with temperature at which samples were heat-treated overnight.....	13
Figure 2-1.	Schematic diagram of the biomathematical model used to describe the retention, distribution and excretion of Pu in dogs, monkeys and rats following inhalation of either $\text{UO}_2 + \text{PuO}_2$, $(\text{U,Pu})\text{O}_2$ or "pure" PuO_2 . Where more than one rate constant is shown for a given pathway, the suffix letter D (dogs), M (monkeys) and (R) (rats) indicates which constant is associated with each species.....	24
Figure 2-2.	Lung retention, tracheobronchial lymph node and liver uptake and retention of Pu in dogs following inhalation of either $\text{UO}_2 + \text{PuO}_2$, $(\text{U,Pu})\text{O}_2$ or "pure" PuO_2 . Data points represent individual dogs whereas curves represent model predictions.....	25
Figure 2-3.	Lung retention, tracheobronchial lymph node and liver uptake and retention of Pu in monkeys following inhalation of either $\text{UP}_2 + \text{PuO}_2$, $(\text{U,Pu})\text{O}_2$ or "pure" PuO_2 . Data points represent individual monkeys whereas curves represent model predictions.....	25
Figure 2-4.	Lung retention, tracheobronchial lymph node and liver uptake and retention of Pu in rats following inhalation of either $\text{UO}_2 + \text{PuO}_2$, $(\text{U,Pu})\text{O}_2$ or "pure" PuO_2 . Data points represent individual rats whereas curves represent model predictions.....	26
Figure 2-5.	Schematic diagram of the biomathematical model used to describe the retention, distribution and excretion of Am in dogs, monkeys and rats following inhalation of either $\text{UO}_2 + \text{PuO}_2$, $(\text{U,Pu})\text{O}_2$ or "pure" PuO_2 . Where more than one rate constant is shown for a given pathway, the suffix letter D (dogs), M (monkeys) and R (rats) indicates which constant is associated with each species.....	26
Figure 2-6.	Lung retention, tracheobronchial lymph node and liver uptake and retention of Am in dogs following inhalation of either $\text{UO}_2 + \text{PuO}_2$, $(\text{U,Pu})\text{O}_2$ or "pure" PuO_2 . Data points represent individual dogs whereas curves represent model predictions.....	27

LIST OF FIGURES (continued)

	<u>Page</u>
Figure 2-7. Lung retention, tracheobronchial lymph node and liver uptake and retention of Am in monkeys following inhalation of either $UO_2 + PuO_2$, $(U,Pu)O_2$ or "pure" PuO_2 . Data points represent individual monkeys whereas curves represent model predictions.....	27
Figure 2-8. Lung retention, tracheobronchial lymph node and liver uptake and retention of Am in rats following inhalation of either $UO_2 + PuO_2$, $(U,Pu)O_2$ or "pure" PuO_2 . Data points represent individual rats whereas curves represent model predictions.....	28
Figure 2-9. Schematic diagram of the biomathematical model used to describe lung retention and uptake and retention in the tracheobronchial lymph nodes of U in dogs and monkeys following inhalation of $UO_2 + PuO_2$ or $(U,Pu)O_2$. Where more than one rate constant is shown for a given pathway the suffix letter D (dogs) and M (monkeys) indicates which constant is associated with each species.....	28
Figure 2-10. Lung retention and tracheobronchial lymph node uptake and retention of U in dogs following inhalation of either $UO_2 + PuO_2$ or $(U,Pu)O_2$. Data points represent individual dogs whereas curves present model predictions.....	29
Figure 2-11. Lung retention and tracheobronchial lymph node uptake and retention of U in monkeys following inhalation of either $UO_2 + PuO_2$ or $(U,Pu)O_2$. Data points represent individual monkeys whereas curves present model predictions.....	29
Figure 3-1. Comparison of dogs that died of radiation pneumonitis and pulmonary fibrosis and monkeys sacrificed after inhalation of mixed oxide aerosols. Symbols are M = monkey sacrificed, D = dog died.....	39
Figure 4-1. Lung retention of $(U,Pu)O_2$ or "pure" PuO_2 in rats.....	43
Figure 4-2. Cumulative percentage survival of rats exposed to graded levels of initial lung burden; a) where inhaled material was $(U,Pu)O_2$ and b) where inhaled material was "pure" PuO_2	44

LIST OF TABLES

	<u>Page</u>
Table 1-1. Comparison of the ratio of adsorbed ^{85}Kr (gamma ray counts) to the ratio of sample weights for two pairs of standard TiO_2 powders.....	8
Table 1-2. Comparison of specific surface area (m^2/g) obtained by ^{85}Kr adsorption and microbalance methods for two samples of UO_2	8
Table 1-3. Replicate determination of the specific surface area (m^2/g) of mono-disperse fused aluminosilicate particulates of two sizes using ^{85}Kr adsorption method.....	8
Table 1-4. Specific surface area values for standard powders determined by three different methods.....	13
Table 1-5. Specific surface area of particulate samples of materials used in fabrication of U and Pu mixed oxide nuclear fuels.....	18
Table 2-1. Measured values for variables in equation describing solubilization of particles deposited in lungs of dogs, monkeys and rats.....	23
Table 3-1. Rats exposed to mixed oxide aerosols that died before scheduled sacrifice times.....	34
Table 3-2. Dogs exposed to mixed (U,Pu) oxide aerosols that died before their scheduled sacrifice times.....	36
Table 3-3. Monkeys exposed to mixed (U,Pu) oxide aerosols and sacrificed longer than one year after exposure.....	37
Table 4-1. Experimental design of dose response studies in Fischer-344 rats that inhaled (U,Pu) O_2 or "pure" PuO_2	42
Table 4-2. Distribution of Pu in tissues of rats sacrificed at selected times after inhalation exposure to (U,Pu) O_2 . Data expressed as percentages (mean \pm 1 SD) of the initial lung burden.....	42
Table 4-3. Distribution of Pu in tissues of rats sacrificed at selected times after inhalation exposure to "pure" PuO_2 . Data expressed as percentage (mean \pm 1 SD) of the initial lung burden.....	43
Table 4-4. Status of dose response studies in which Fischer-344 rats were exposed to graded ILB levels of either (U,Pu) O_2 or "pure" PuO_2 (on June 30, 1982).....	45
Table 4-5. Summary of histopathologic findings in rats exposed to aerosols of mixed oxides and dying before April 1, 1982.....	46

ACKNOWLEDGEMENTS
PERSONNEL CONTRIBUTING TO THE RESEARCH

Senior and Associate Staff

J. A. Mewhinney	Ph.D.	Radiobiologist
B. B. Boecker	Ph.D.	Radiobiologist
A. F. Eidson	Ph.D.	Chemist
D. H. Gray	M.S.	Radiochemist
F. F. Hahn	D.V.M., Ph.D.	Experimental Pathologist
S. J. Rothenberg	Ph.D.	Aerosol Scientist
H. C. Redman	D.V.M., M.P.V.M.	Research Veterinarian

Technical Staff

M. F. Conrad	Laboratory Technician
J. L. Casaus	Radiochemistry Analyst
J. A. Romero	Laboratory Technician

It should be emphasized that a listing such as this is rarely comprehensive in acknowledging individuals who have made important contributions to the research. In the unnamed category are the many highly skilled animal care, maintenance, shop, administrative and secretarial personnel whose efforts are essential to the continuation of a productive and meaningful research project. Research is performed in facilities fully accredited by the American Association for the Accreditation of Laboratory Animal Care.

EXECUTIVE SUMMARY

This annual progress report details the research conducted in the project, "Radiation Dose Estimates and Hazard Evaluations for Inhaled Airborne Radionuclides." The report is composed of a series of four research papers, each presenting the status of specific areas of the total research effort. An attempt has been made to include substantial detail in each paper to indicate clearly the state of the research and to provide interpretation of the results where possible. The reader is advised that in many cases these interpretations are preliminary; and final, more complete interpretations and comparison must await the completion of individual research projects.

The objective of this project is to conduct confirmatory research on aerosol characteristics which may modify the biological fate, patterns of radiation dose and predicted health consequences of airborne radioactivity which may be released in normal operations or under accident conditions in the nuclear fuel cycle. It involves physical, chemical and biological characterization of aerosol actually present in different segments of the nuclear fuel cycle. Since it involves actual aerosols produced in industrial operations, this work provides a key link between studies with idealized, laboratory-produced aerosols and derived radiation protection standards and hazard analyses. Industrially-collected aerosol materials are reaerosolized in the laboratory to determine the patterns of deposition, retention and translocation in laboratory animals as a function of time after an inhalation exposure. The aerosols used for these studies are characterized using a number of physical and chemical techniques to determine possible differences between the aerosol and the corresponding bulk material which might help to explain the observed patterns seen in the animals after exposure. Multiple species (rats, dogs and monkeys) are being used to strengthen the eventual extrapolation to man. Although current studies are concentrated on the biological characterization of mixed (UO_2 , PuO_2) fuel elements, later studies may utilize materials from other sources of industrial operations involving the handling of nuclear fuel material as well as from the pilot processes involved in fabrication or processing advanced fuel forms.

The research reports begin with a paper, presented in three parts, which provides complete details regarding the development of a method for determination of the specific surface area of small samples of highly radioactive particulates. The first part of the three-part paper describes the development of an apparatus, housed within a glove box, in which the particulate sample is first outgassed under vacuum and heating to $\sim 280^\circ\text{C}$ to remove adsorbed water from the surface, then ^{85}Kr is admitted to the sample holding container and the ^{85}Kr adsorbs to the surface of the particulates in a monolayer. The final stage in the determination is quantifying the amount of ^{85}Kr adsorbed on the particulates using gamma ray counting. The second part of the three-part paper details the results of two intercomparisons; a comparison of the results obtained using three different methods of quantifying the amount of gas adsorbed onto particle surfaces and a second comparison of three different particulate materials to determine their respective suitability for use as specific surface area standards. These comparisons were made to provide essential quality assurance information. The results of these intercomparisons clearly indicate that while all three methods provide results differing only within experimental error, only the ^{85}Kr method provides simultaneously the ability to safely contain highly radioactive particulate samples and to characterize reliably samples as small as ~ 2 mg. Comparison of the standard powder samples indicated that the Al_2O_3 was most suitable since the measured specific surface area was not effected by outgassing temperatures up to 250°C . The third part of this three-part paper describes the acquisition of specific surface area data for particles of $\text{UO}_2 + \text{PuO}_2$ treated at 750°C , two samples of $(\text{U,Pu})\text{O}_2$ treated at 1750°C , and "pure" PuO_2 treated at

850°C. These particulate samples were recovered from membrane filter samples taken during the inhalation exposure of rats, dogs and monkeys in the radiation dose pattern or dose-response studies conducted in this project. Replicate determinations on each sample produced consistent results for two of the samples; specific surface area of $\sim 3 \text{ m}^2/\text{gm}$ for one $(\text{U,Pu})\text{O}_2$ sample and $\sim 20 \text{ m}^2/\text{gm}$ for "pure" PuO_2 . For two other materials, $\text{UO}_2 + \text{PuO}_2$ and one $(\text{U,Pu})\text{O}_2$ sample, the specific surface area increased for several determinations made successively on the same sample. Potential causes for this phenomenon are discussed.

The second paper in this report discusses the application of a biomathematical model to describe retention, distribution and excretion of Pu, Am and U in rats, dogs and monkeys following inhalation of $\text{UO}_2 + \text{PuO}_2$, $(\text{U,Pu})\text{O}_2$ or "pure" PuO_2 . The model, which uses the specific surface area of the inhaled particulates in the formulation of a function to describe the rates of dissolution of these elements, provides good agreement with the observed retention and distribution data for Pu for all three species studied. Results of these modeling efforts indicate that for a given element, slight differences in the retention, distribution and excretion of that element for a given species can be accounted for by the differences in the physical chemical characteristics of the aerosol. For a given aerosol, significant differences in retention, distribution and excretion were noted among the three animal species. Also, for each species, differences were found in the retention, distribution and excretion of the elements Pu, Am, and U (when present) for each aerosol.

The third paper in this report summarizes the biological effects (response) observed in rats, dogs and monkeys held for long periods after inhalation exposure to $\text{UO}_2 + \text{PuO}_2$, $(\text{U,Pu})\text{O}_2$ or "pure" Pu. These effects include lung tumors induced in both rats and dogs experiencing lung doses from 190 to 16,000 rads in rats and from 2,500 to 4,800 rads in dogs. None of the three monkeys sacrificed at four years after inhalation had developed tumors with lung doses ranging from 2,900 to 4,700 rads. A full discussion of the tumor types observed in rats and dogs is presented.

The fourth paper in this report provides an interim report on the dose-response studies being conducted in Fischer-344 rats exposed to aerosols of $(\text{U,Pu})\text{O}_2$ or "pure" PuO_2 . In these ongoing studies, groups of rats were exposed to three graded levels of initial lung burden to achieve total doses to lung of 25, 125 and 625 rads to 950 days after exposure. Relatively few rats have succumbed to radiation related lesions to date as expected. A few pulmonary tumors have been observed in the high dose groups. Data on the retention and distribution of these materials through 1.5 years are presented as a summary of the histopathological responses seen to date.

1. SURFACE AREA MEASUREMENTS

PART A. MEASUREMENT OF SPECIFIC SURFACE AREAS OF SMALL POWDER SAMPLES USING ⁸⁵Kr AS ADSORBATE

Abstract — An apparatus is described which has been successfully employed for measurement of the specific surface area of particulate samples weighing between 20 and 50 mg. Comparison of data obtained for 50 mg samples by the new method with data obtained for the same samples by other methods is made in Part B. A ratio test was employed to demonstrate that the method gives self-consistent data for samples less than 10 mg. The blank correction is $20 \text{ cm}^2 \pm 10 \text{ cm}^2$, the uncertainty in weighing samples is $\pm 0.05 \text{ mg}$. Sample tubes are suitable for containment of radioactive material. Application of the methods to 2.0 and 10 mg mixed PuO_2/UO_2 samples obtained from gloveboxes in a nuclear fuel fabrication facility is presented in Part C.

PRINCIPAL INVESTIGATORS

S. J. Rothenberg
D. K. Flynn
A. F. Eidson
G. J. Newton
J. A. Mewhinney

Important factors determining the rate of dissolution of a particle deposited in the lung are the chemical composition of the particle, the crystalline structure and the amount of surface interacting with body fluids. This paper describes work designed to allow measurements of specific surface area for extremely small samples of radioactive particles. Several commercial methods are available for determination of specific surface area of particles, but these are limited to sample sizes exceeding 10 mg (Ref. 1). Particulate samples from filters, cascade impactors or the Lovelace Aerosol Particle Separator (LAPS) (Ref. 2) are normally available in quantities between 0.1 mg and 10 mg, and thus development of a method suitable for such small samples was necessary.

This paper describes the adaptation of a method for measurement of the specific surface area described by Chenebault and Schurenkamper (Ref. 3) for powder samples. Comparison of the method with other methods of measurement of specific surface area is described in Part B, and application of this new method to measurement of specific surface area of particulates of mixed U and Pu oxides of industrial origin is described in Part C.

MATERIALS

Samples of titanium dioxide and aluminum oxide of uniform composition and known specific surface area were obtained from Duke Standards Co., Palo Alto, California. Nominal specific surface areas of each batch, as supplied, were checked using a vacuum micro-balance for gravimetric determination of adsorption of nitrogen, and the method of calculation of Brunauer, Emmett and Teller (six-point B.E.T. plot) (Ref. 4). The gravimetric method has been discussed elsewhere (Ref. 5) and the apparatus described in detail (Ref. 6). Uranium dioxide (Merck analytical standard) was used without further purification. Fused aluminosilicate particles (FAP) were produced from montmorillonite clay (Ref. 7) and separated into size-selected samples using a Lovelace Aerosol Particle Separator (LAPS). Samples of mixed oxides of U and Pu were obtained from two different fuel fabrication facilities (Ref. 8, 9, 10).

The apparatus consisted of a vacuum manifold to which adsorption cells and a reservoir of ⁸⁵Kr were attached and a pumping assembly capable of producing a vacuum of 10^{-6} Torr. A

schematic diagram of the apparatus is shown in Figure 1-1. Ancillary equipment included heating assemblies, heater control units and pressure gauges, and adsorption cells. A capacitance manometer (MKS type HSIA) was used to measure the pressure of ^{85}Kr .

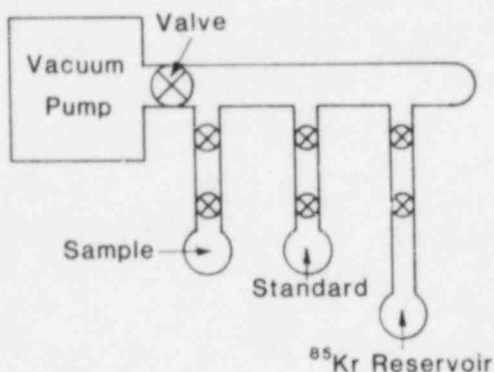


Figure 1-1. Schematic diagram of ^{85}Kr adsorption apparatus. A sample and a standard powder of known specific surface area are attached to the vacuum manifold. The system is evacuated to 10^{-5} Torr and the sample and standard powder heated to 250°C for ~ 16 hours. Krypton-85 is then admitted from the reservoir and the sample and standard powders adsorb ^{85}Kr when cooled in liquid nitrogen. Taps to sample and standard powder cells are closed and the cells removed to a counting station to quantify the ^{85}Kr adsorbed.

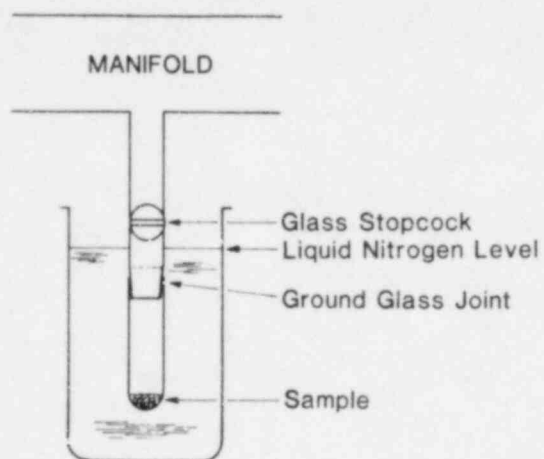
Three types of adsorption cells were employed. The simplest consisted (Fig. 1-2a, type I cell) of a plain tube, approximately 6" long, internal diameter = $1/2$ ", ending in a $14/35$ standard taper ground glass male joint which was inserted into a $14/35$ female joint attached to a stop-cock (and thus sealed once a sample was placed in it). The entire sealed assembly was then transferred from the glove box used for sample storage to the glove-box housing the surface area measurement apparatus, and attached to the vacuum manifold. Type I cells were inexpensive and easy to load, but were suitable only for large (~ 50 mg) samples because of the large blank correction whose value depends on the level of liquid nitrogen cooling the adsorption cell and its contents.

A cell not suffering from this disadvantage, which is a variant on the design of Chenebault, (Ref. 3) is shown in Figure 1-2b (type II cell). A partially evacuated envelope was joined to the cell (Ref. 1) that allowed the liquid nitrogen level to vary between points A and B (Fig. 1-2b) but maintained constant cooling below point B such that the blank correction was almost constant. This cell was also easy to load and seal, had a much lower blank correction and gave good results for samples as small as ~ 5 mg and specific surface area of at least $1\text{ m}^2\text{g}^{-1}$. The type II cell weighed ~ 6 g, which was just outside the range of several commercially available digital readout balances weighing to $\pm 1\text{ }\mu\text{g}$. However, a type II cell could be made which weighed less than 4 g without the stop-cock. Using a balance in a controlled area (e.g. glove-box), the contents of such a cell could be weighed open to $\pm 1\text{ }\mu\text{g}$, a fiftyfold improvement in weighing precision to that reported below (see Results).

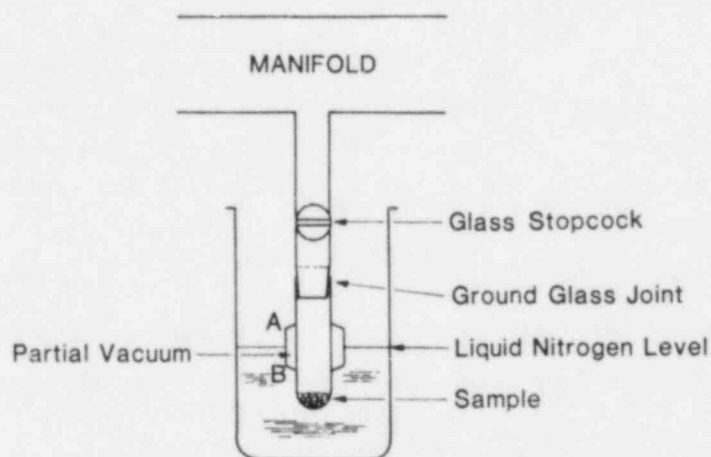
The dead-space correction for a type II cell was determined by the total volume enclosed with the stop-cock shut. The dead-space correction was significant using ^{85}Kr as adsorbate. Thus, reduction in both cell diameter and length improved precision of the method. It was difficult to load powder samples into cells with less than 2 mm inside diameter. Type II cells were at least $5\text{ }1/2$ " long. This was because it was necessary to leave ~ 1 " between the barrel of the stop-cock and the ground glass joint, and because the joint itself was ~ 1 " long.

The type III cell design eliminated the ground glass joint (Fig. 1-2c). The total cell length was ~ 3 ". The bore of the stop-cock was carefully widened out to facilitate sample loading with a special mini-spatula. Such cells were difficult to make and to load, but were used to obtain reproducible data for samples as small as 2.0 mg ($S \geq 1\text{ m}^2\text{g}^{-1}$).

A



B



C

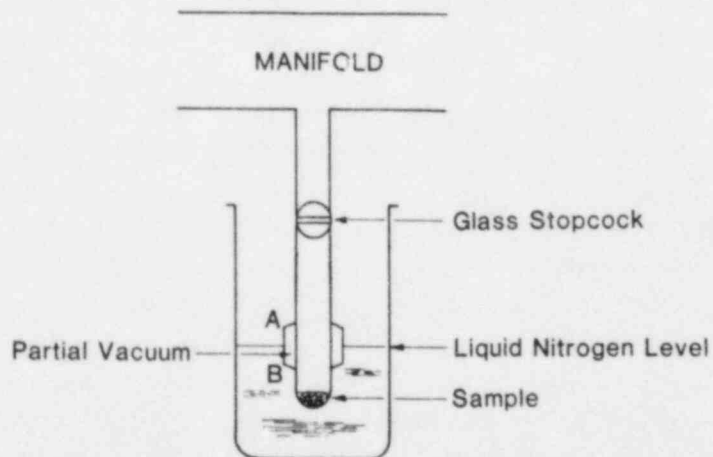


Figure 1-2. Sample and standard powder cells used for ^{85}Kr adsorption; a) type I cell, b) type II cell and c) type III cell. In type II and III cells, the amount of glass cooled sufficiently to adsorb ^{85}Kr is nearly independent of the liquid nitrogen level provided it is between points A and B.

Both Kr and Xe are standard adsorbates used in surface area determinations (Ref. 5, 11). Both radionuclides are easily determined radiometrically, having distinct gamma ray energies. The half-life of ^{85}Kr is about 10 years, whereas that of ^{133}Xe is only about 5 days.

A vacuum apparatus can be easily assembled from standard components and quick disconnect O-ring seals which provides a pressure of 10^{-5} - 10^{-7} Torr (for outgassing) and an overall leak-rate of less than 10^{-3} Torr min^{-1} . This specification is adequate if ^{85}Kr is used as an adsorbate, since the working pressure range for ^{85}Kr adsorption studies at 77°K is ~ 0.1 - 0.5 Torr. It also ensures that at the end of an adsorption experiment (~ 1 hour) less than 2% of the pressure measured is caused by extraneous air, and that the background pressure at the start of an experiment is less than 0.1% of the ^{85}Kr admitted. With ^{133}Xe as adsorbate, and a working pressure range of $\sim 10^{-4}$ Torr at 77°K, a better ultimate vacuum ($\sim 10^{-8}$ Torr) and lower leak rate ($\sim 10^{-8}$ Torr min^{-1}) would be essential. Other precautions, such as vacuum bake-out of all components to minimize outgassing, are necessary, as discussed by Chenebault (Ref. 3).

The dead-space correction previously mentioned was determined by the product of cell volume and working gas pressure. A type II cell would be acceptable for submilligram samples ($S \geq 1 \text{ m}^2 \text{ g}^{-1}$) if ^{133}Xe was used as adsorbate with working gas pressure of $\sim 10^{-4}$ Torr. An "ultra-high" vacuum system then becomes essential, but this advantage might be outweighed by the convenience of using type II cells. Because of the short half-life of ^{133}Xe and the need for an ultra-high vacuum system, we used ^{85}Kr as the adsorbate in this work.

METHODS

As much of each sample as could be removed from each sampling filter, cascade impactor stage or LAPS foil segment was placed in a preweighed sample tube (Fig. 1-2). An approximately equal weight of titanium or aluminum oxide standard powder was placed in a second preweighed sample tube. Both tubes were reweighed on a Mettler type H51 balance. Sample, standard and an identical clean empty sample tube (blank) were transferred into the glove box and attached to the vacuum manifold (Fig. 1-1). A reservoir of ^{85}Kr was also attached to the vacuum manifold, and the apparatus slowly pumped down to 10^{-6} Torr. Throttling valves (not shown) were employed to ensure that the powder samples were not aerosolized when the pumps were switched on. These procedures have been discussed in detail elsewhere (Ref. 1, 12). Samples, standard and blank were heated overnight at 250°C and 10^{-6} Torr. Temperature was controlled to $\pm 5^\circ\text{C}$ by proportioning controllers and monitored to $\pm 1^\circ\text{C}$ by a fast-response thermocouple (Type J, 1/8" o.d.) placed next to the sample tube.

After heating overnight, samples were allowed to cool to room temperature at 10^{-6} Torr, 0.5 Torr of ^{85}Kr was admitted to the apparatus from the ^{85}Kr reservoir, and sample, standard and blank were simultaneously cooled in liquid nitrogen, to adsorb the ^{85}Kr . When adsorption was complete, as indicated by constant pressure readings (M.K.S. Type 222 baratron) the taps to the sample cells were shut, ^{85}Kr in the manifold was returned to the reservoir. The reservoir was removed to a shielded well in a second glove-box to reduce background for later measurement. Sample, standard and blank cells were placed, in turn, in a counting station. The amount of ^{85}Kr adsorbed by sample, standard and blank were determined by counting the 0.514 MeV gamma ray using a 1" NaI(Tl) crystal detector and a Ludlum model 2200A scaler attached to an automatic printing unit. The mean of four 2-minute counts was obtained for each cell, and the cell was removed and replaced in the counting unit two more times to check that counting geometry was reproducible. The specific surface area of the sample was then determined by the equation:

$$\frac{S_1 W_1}{S_0 W_0} = \frac{\text{Mean Net Counts}_1}{\text{Mean Net Counts}_0} \quad (\text{Eq. 1-1})$$

where S_1 and W_1 are the specific surface area and weight of the sample, S_0 and W_0 the specific surface area and weight of the standard. Net Counts₁ and Net Counts₀ are the counts obtained for sample and standard. Correction was made for both detector background and blank cell counts, and care taken to ensure that reproducible counting geometry was obtained.

The same procedures were followed in a cross-check on the method using the vacuum micro-balance. The specific surface area of each sample was first determined on the vacuum microbalance by gravimetric methods (Ref. 6) and the sample then transferred from the vacuum micro-balance pan to the weighed sample tube. Depleted uranium dioxide was used in these studies, as the vacuum microbalance was not modified for containment of radioactive samples. This cross-check employed large samples (50 mg) to obtain reliable results by the gravimetric method.

To ensure that a single sample gave consistent results after repeated outgassing periods, three repeated measurements were made on monodisperse fused aluminosilicate particulates (FAP), a material known to be heat stable at 250°C. This test procedure was repeated at intervals.

In a further cross-check on the ^{85}Kr method, sample and standard cells were filled with different weights of titanium dioxide taken from the same batch. Except that both cells contained samples of the same kind, the procedures followed were identical to those used for mixed oxide determinations.

RESULTS

Comparisons of sample weight ratios to ^{85}Kr gamma-count ratios for TiO_2 samples are shown in Table 1-1. Comparison of specific surface areas obtained using the vacuum micro-balance and by ^{85}Kr adsorption for uranium dioxide samples are shown in Table 1-2. The specific surface areas for two different particle sized monodisperse samples of FAP after three successive outgassing periods are shown in Table 1-3.

DISCUSSION

If the samples obtained from Duke Standards are homogenous with respect to surface area, then equation (1-1) reduces to:

$$\frac{W_1}{W_2} = \frac{\text{Counts}_1}{\text{Counts}_2} \quad (\text{Eq. 1-2})$$

Two pairs of TiO_2 samples were compared: (1) 50 mg and 25 mg samples (Pair A) and (2) 10 mg and 5 mg samples (Pair B). If the correction for adsorption by the sample tubes (blank correction) is omitted, then the weight ratios and gamma-count ratios agree to within 10% for Pairs A and B. When blank corrections are included in the calculation, agreement to within 5% is obtained, which is within the expected precision of the method. (Ref. 1,5) As discussed by Lowell et al., (Ref. 13) who examined the minimum sample size for the flowing gas method, an apparatus which gives self-consistent data for large samples may show a systematic trend in data as sample size is reduced. The data in Table 1-1 demonstrate that, provided the blank correction is applied, the ^{85}Kr method is self-consistent for TiO_2 samples as small as 5 mg. Additional measurements of U and Pu oxides demonstrated that the method was satisfactory for samples as small as ~ 2 mg (this report, pp. 16 to 20).

Table 1-1. Comparison of the Ratio of Adsorbed ^{85}Kr (Gamma ray Counts) to the Ratio of Sample Weights for Two Pairs of Standard TiO_2 Powders

	Weight (mg)	Counts (cpm) (No Blank Correction)	Counts (cpm) (With Blank Correction)
Pair A			
Sample A-1	50	157000	137000
Sample A-2	25	87100	67400
Ratio	2.0:1	1.8:1	2.0:1
Pair B			
Sample B-1	10.84	22700	21100
Sample B-2	5.88	13600	12000
Ratio	1.84:1	1.67:1	1.76:1

Table 1-2. Comparison of Specific Surface Area (m^2/g) Obtained by ^{85}Kr Adsorption and Microbalance Methods for Two Samples of UO_2

Sample	^{85}Kr	^c Microbalance
1	3.3 ^a 3.6 ^b	3.56
2	4.2	3.64
Mean	3.7	3.60

^aFirst determination

^bSecond determination

^cMean of determinations from adsorption and desorption isotherms

Table 1-3. Replicate Determination of the Specific Surface Area (m^2/g) of Monodisperse Fused Aluminosilicate Particulates of Two Sizes Using ^{85}Kr Adsorption Method

Particle Size (μm)	Sample Weight (mg)	Determination			Mean \pm 1 SD
		1	2	3	
1.3	7.42	2.67	2.54	2.67	2.63 \pm 0.08
0.9	5.00	2.59	2.79	2.57	2.65 \pm 0.12

The specific surface area of replicate uranium dioxide samples determined on the vacuum micro-balance (Table 1-2) was $3.6 \pm 0.1 \text{ m}^2 \text{ g}^{-1}$, whereas a value of $3.7 \pm 0.6 \text{ m}^2 \text{ g}^{-1}$ was determined using adsorption of ^{85}Kr and a plain tube cell (Fig. 1-2a) able to hold 50 mg samples. These results indicated that the method gave results agreeing within the limits of detection. The manufacturer's specification for this sample did not include homogeneity with respect to either particle size or specific surface area. Thus it was not immediately clear whether the apparent difference between the two UO_2 samples was real, or represented scatter in the data.

Subsequent work showed that the uncertainty in blank correction for type I cells was as great as the difference between the ^{85}Kr and the vacuum microbalance data for UO_2 samples. To obtain reliable results in such a cross-check it is essential to transfer over 30% of the sample from the micro-balance pan to the sample tube. In addition, it was noted that as the UO_2 samples were heated through the temperature range 100°C - 200°C (at 10^{-5} Torr), an irreversible weight gain occurred. This was presumably caused by partial oxidation of UO_2 to U_3O_8 , which has been observed by others (Ref. 14). The weight gain implied that the material chosen (UO_2) would not necessarily be in the same physical state at the end of a series of experiments as at the start, and that the differences in data might reflect a real change in the sample. Further cross-checks were deferred until the precision of the ^{85}Kr method had been improved, and experience gained in use of the ^{85}Kr method before the data for aluminum oxide (Part B) was obtained.

The method gave reproducible results when a heat-stable sample and a type III cell was used. When roughness factors were calculated from the specific surface areas and the sizes of the FAP particles (determined by transmission electron microscopy), values for successive batches of FAP ranged from 1.1 to 1.75 with a mean of 1.4. The appearance of the particles is one of smooth spheres. The range reported is somewhat wider than that summarized by Gregg and Sing (Ref. 5) for smooth surfaces. Gregg and Sing reviewed the literature and found a range 1.05 to 1.4. The departure from a value of 1.0 was attributed to small surface irregularities, such as lattice steps, lack of short-range order in crystallites or lattice defects. If a "correct" value for FAP of ≈ 1.2 is assumed, then the data indicate a systematic error of $\approx 20\%$, and random errors of $\pm 30\%$. Thus, the method had been found to be self-consistent, free from gross systematic error, and to give reproducible results. We were therefore encouraged to proceed to a more detailed evaluation of standards and comparison with other methods as described in Part B, and to apply the method to mixed oxide samples as described in Part C.

SUMMARY

An apparatus suitable for the determination of the specific surface area characterization of small masses of particulates requiring containment has been constructed. The method gives self-consistent data for samples between 2 and 50 mg. The method has also been tested against other methods (Part B) and applied to (Pu/U) oxide samples (Part C).

REFERENCES

1. Rothenberg, S. J., P. B. DeNee, Y. S. Cheng, R. L. Hanson, H. C. Yeh and A. F. Eidson, "Methods for the Measurement of Surface Areas of Aerosols by Adsorption," Adv. Colloid Interface Sci. 15: 223-249, 1982.
2. Kotrappa, P. and M. E. Light, "Design and Performance of the Lovelace Aerosol Particle Separator," Rev. Sci. Instrum. 43: 1106, 1972.

3. Chenebault, P. and A. Schürenkämper, "The Measurement of Small Surface Areas by the B.E.T. Adsorption Method," J. Phys. Chem. 69: 2300, 1965.
4. Brunauer, S., P. H. Emmett and E. Teller, "Adsorption of Gases in Multi-Molecular Layers," J. Am. Chem. Soc. 60: 309, 1938.
5. Gregg, S. J. and K. S. W. Sing, "Adsorption, Surface Area and Porosity," Academic Press, New York, 1967.
6. Rothenberg, S. J., "Coal Combustion Fly Ash Characterization: Adsorption of Nitrogen and Water," Atmos. Environ. 14: 445, 1980.
7. Raabe, O. G., G. M. Kanapilly and G. J. Newton, "New Methods for the Generation of Aerosols of Insoluble Particles for Use in Inhalation Studies," in Inhaled Particles III, Proceedings of an International Symposium, British Occupational Hygiene Association, pp. 3-18, September 14-23, 1970.
8. Raabe, O. G., G. J. Newton, C. J. Wilkinson, S. V. Teague, and R. C. Smith, "Plutonium Aerosol Characterization Inside Safety Enclosures at a Demonstration Mixed-Oxide Fuel Fabrication Facility," Health Phys. 35: 649, 1978.
9. Newton, G. J., "Mixed-Oxide Fuel Fabrication," in Radiation Exposure and Risk Estimates for Inhaled Airborne Radioactive Pollutants Including Hot Particles - Annual Report for Period 1 July 1976 to 30 June 1977, NUREG/CR-0010, available from National Technical Information Service, Springfield, VA, 1978.
10. Stanley, J. A. and G. J. Newton, "Further Sampling of Aerosolized Mixed-Oxide Nuclear Fuel in a Fabrication Facility," in Radiation Dose Estimates and Hazard Evaluations for Inhaled Airborne Radionuclides - Annual Report for Period 1 July 1977 to 30 June 1978, NUREG/CR-0673, available from National Technical Information Service, Springfield, VA, 1979.
11. Campbell, K. C. and S. J. Thompson, "Radioisotopes in Studies of Chemisorption and Catalysis," Prog. Surf. Membrane Sci. 9: 163-221, 1975.
12. Rothenberg, S. J., A. F. Eidson, G. J. Newton and J. A. Mewhinney, "Use of ⁸⁵Kr to Determine Specific Surface Area of Samples Requiring Glove Box Containment," in Inhalation Toxicology Research Institute Annual Report for 1980-1981, LMF-91, UC-48, 1982*.
13. Lowell, S., and S. Karp, "Determination of Low Surface Areas by the Continuous Flow Method," Anal. Chem. 44: 2395, 1972.
14. Cordfunke, E. H. P., The Chemistry of Uranium, Elsevier, New York, 1969.

*Available for purchase from NRC/GPO sales program, U. S. Nuclear Regulatory Commission, Washington, DC, 20545 or from the National Technical Information Services, Springfield, VA 22161.

1. SURFACE AREA MEASUREMENTS

Part B. A COMPARISON OF THREE METHODS OF DETERMINING SPECIFIC SURFACE AREA AND A COMPARISON OF THREE MATERIALS FOR SURFACE AREA STANDARDS

Abstract — Specific surface areas of three standard particulate samples were measured by vacuum micro-balance, flowing gas thermal conductimetric method and ^{85}Kr adsorption techniques. Values obtained were found to be independent of the method employed, or of the operator using the

equipment, but to be influenced by the temperature at which samples were heated (outgassed) prior to determination of adsorption properties. Implications for comparison of data for environmental samples characterized in different laboratories are discussed, and the suitability of the materials tested as surface area standards evaluated.

PRINCIPAL INVESTIGATORS

S. J. Rothenberg

J. A. Mewhinney

A. F. Eidson

D. K. Flynn

During our studies of the surface properties of respirable particles from different sources we have sought to compare our results to data obtained for similar samples studied at other laboratories (Ref. 1, 2, 3, 4). Data for chemical composition show considerable particle to particle variation (Ref. 4, 5, 6, 7), but few major discrepancies between data from different laboratories, and therefore will not be further discussed. The situation for adsorption studies is somewhat less satisfactory (Ref. 1, 2, 3). Frequently, systematic differences in data obtained at different laboratories can be explained by intentional differences in sampling method or experimental approach. Gregg and Sing (Ref. 8) recommend heating samples to constant weight at temperatures in excess of 200°C (to remove adsorbed surface impurities, or "outgas" the sample) before studying adsorption properties. This approach is excellent for heat-stable samples such as well-characterized oxide catalysts. For ambient air samples, which may include heat-labile particles, there are compelling reasons for studying samples as collected, without preliminary outgassing (Ref. 3). If sufficient samples are available, it is desirable to use both experimental approaches, but data obtained by the two methods cannot readily be compared nor expected to be concordant. In addition, different laboratories may use apparatus based on different measurement principles.

In this paper, we compare three different methods of determining specific surface area of particulate samples, all of which employ gas adsorption techniques, but use very different methods of determining the amount of gas adsorbed. To minimize effects of differences in sample preparation (outgassing) we have outgassed non-heat-labile samples overnight at 250°C. The methods compared are gravimetric (vacuum micro-balance), thermal conductimetric flowing gas technique (Ref. 9) (Quantasorb) and a radiometric technique employing ^{85}Kr adsorption. The ^{85}Kr adsorption method, described in Part A, is the only method which gives reliable data, if the total sample mass available is less than 2 mg, and provides convenient containment of radioactive samples. However, as presently employed, it provides a single point determination in which the method of calculation of Brunauer, Emmett and Teller is used (BET method) (Ref 10) for two samples a day. The flowing gas thermal conductimetric method is very useful for samples weight at least 20 mg as five-point B.E.T. plots for four samples can be obtained in a single day. In addition, the latter system can be used to determine hysteresis loops and pore size distributions (Ref. 11). The gravimetric technique can be used to study weight loss curves (Ref. 3), rates of adsorption and desorption (Ref. 2, 3) (or sorption kinetics), and isothermic heats of

adsorption as well as for the routine B.E.T. determination of specific surface area (Ref. 1, 3). Thus, the gravimetric technique is particularly useful for the in-depth study of a few samples. The advantages and disadvantages of each method have been recently reviewed (Ref. 12). Since we wish to use the most appropriate technique for each sample and yet be able to compare surface area data from different samples, we carried out a comparison of the three methods. In addition, since the ^{85}Kr method depends on the use of a standard sample, we have compared two materials (Al_2O_3 and TiO_2) available as specific surface area standards.

As reported below, we found Al_2O_3 somewhat more satisfactory than TiO_2 as a specific surface area standard material, since the values obtained were almost independent of the heat treatment used during sample outgassing. Differences in data obtained by the three methods usually were greater than $\pm 5\%$ but less than $\pm 10\%$. This means that data obtained by different laboratories using the same method of sample preparation but different measurement techniques should be directly comparable.

EXPERIMENTAL DESIGN

Three samples of alumina oxide of widely differing specific surface areas were ordered from Duke Standards, Palo Alto, California. A staff member not involved in the hands-on experimental work divided each bottle into two aliquots, labeled them A_1 , A_2 , B_1 , B_2 , etc., gave out the samples for determination of specific surface area by each method, and recorded the results handed back to him. The original experimental design was a "triple blind" experiment, but as a result of changes in personnel, most of the experiments by ^{85}Kr adsorption and by Quantasorb were carried out by a single individual.

As a check on sample inhomogeneities of the type previously reported (Ref. 1), two different subsamples of Al_2O_3 were determined using the vacuum micro-balance. This was also done for TiO_2 samples, since it is necessary to establish that a sample is homogenous with respect to specific surface area if it is to be used as a standard.

MATERIALS AND METHODS

Samples of Al_2O_3 and TiO_2 were obtained from Duke Standards, Palo Alto, California. A vacuum microbalance (Cahn RG2000) was used for gravimetric determination of adsorption of research grade nitrogen (Mattheson). The apparatus and experimental precautions used have been previously described in detail (Ref. 1). A standard Quantasorb instrument was employed in accordance with the manufacturers instructions, using 1%, 5% and 10% research grade nitrogen in helium mixtures (Scientific Gas Co.) and research grade nitrogen (Mattheson Gas Co.). Desorption peak areas were used in all determinations, as recommended by Nelson and Eggertsen (Ref. 9) and by the manufacturer. The standard method of calculation (on data sheets supplied with the instrument) was corrected for the altitude at Albuquerque (barometric pressures ranging from 615-635 mmHg). The ^{85}Kr adsorption technique has been described in detail in Part A.

Duplicate micro-balance determinations were made on each sample, and both adsorption and desorption isotherms measured. Thus, the values tabulated are the mean of four determinations. Quantasorb and ^{85}Kr adsorption experiments were performed in triplicate. To study the effects of heat treatment of samples, successive determinations were made after heating samples overnight at 100°C, 200°C, 250°C, 300°C for Quantasorb and ^{85}Kr and additionally at 450°C for the micro-balance, which has heat resistant (quartz or ceramic) components.

RESULTS

Values obtained after heat treatment at 250°C by vacuum micro-balance, Quantasorb and ^{85}Kr , as well as the specification for each sample supplied by the manufacturer, are shown in Table 1-4. Figure 1-3 shows the dependence of the measured specific surface area on outgassing temperature. For comparison with the standard, materials data previously published for diesel exhaust particles and for coal combustion fly ash are also reproduced in Figure 1-3.

Table 1-4. Specific Surface Area Values For Standard Powders
Determined by Three Different Methods

Sample	Specific Surface Area, m^2g^{-1}			Manufacturer's Specifications
	Micro-balance	Quantasorb	Adsorption ^{85}Kr ^a	
Al_2O_3 , A	2.6	2.53	3.23	3.04 ± 0.25 ^b 3.09 ± 0.24 ^c
Al_2O_3 , B	81.9	76.0	90	81.4
Al_2O_3 , C	13.0	12.6	12.6	14.0
TiO_2	8.85	8.95		10.3

^a TiO_2 used as a standard with value $8.9 \text{ m}^2\text{g}^{-1}$ at 250°C.

^b N_2

^c Kr

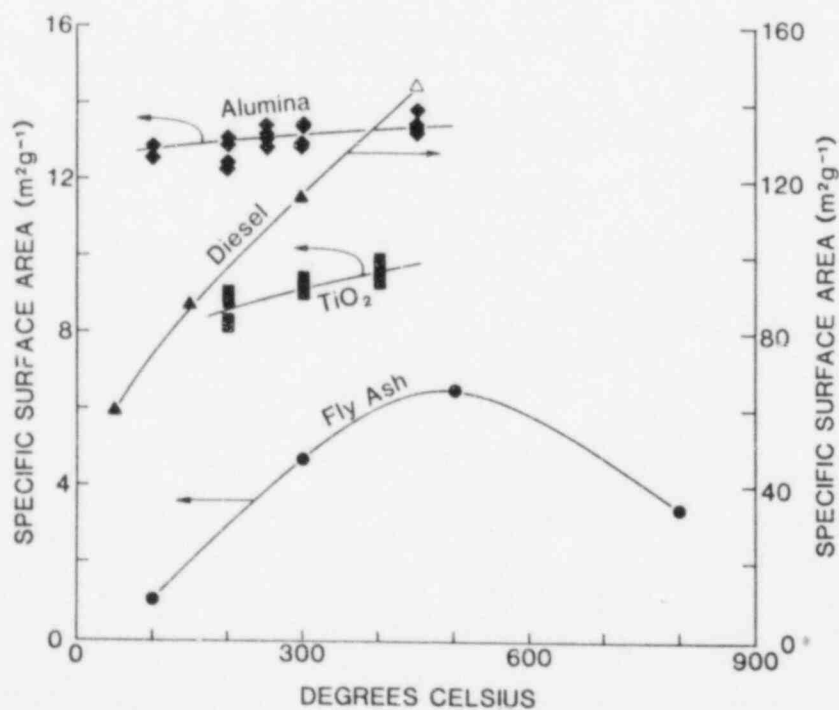


Figure 1-3 Variation of specific surface area with temperature at which samples were heat-treated overnight.

DISCUSSION

The values in Table 1-4 demonstrate good agreement between the three methods. The apparent precision of the ^{85}Kr adsorption method is somewhat less satisfactory ($\pm 10\%$) than that of the other two methods ($\pm 5\%$). This is expected when comparing single point B.E.T. determinations with multi-point B.E.T. determinations. There is no evidence of systematic error in the ^{85}Kr adsorption method. Since the ^{85}Kr adsorption of samples as small as one mg ($S \geq 1 \text{ m}^2 \text{ g}^{-1}$) can readily be determined, this makes it the method of choice for small samples.

A test of the type described herein requires homogenous samples. This is the reason why we used pure laboratory standards, rather than "realistic" filter samples from exposure aerosols. Table 1-2 (Part A), obtained early in the development of the ^{85}Kr method, illustrates this. At the time the ^{85}Kr data were obtained, we had no real way of ascertaining whether the differences in data for the UO_2 samples represented a real difference in subsamples, or greater scatter in data for the ^{85}Kr method than for the vacuum micro-balance method. Subsequent work established that the blank correction was greatly reduced by using Chenebault's sample tube design (Ref. 12, 13). This improved the precision of the ^{85}Kr data. To test the homogeneity of one of the Al_2O_3 samples, we measured the specific surface area of two aliquots by vacuum micro-balance, and obtained values of $80 \text{ m}^2 \text{ g}^{-1} \pm 2 \text{ m}^2 \text{ g}^{-1}$ and $82 \text{ m}^2 \text{ g}^{-1} \pm 2 \text{ m}^2 \text{ g}^{-1}$. Thus, within the limits of detection of the method used, the sample appeared to be homogenous with respect to surface area. In a similar check on two aliquots of the TiO_2 standard, values of 8.7 and $9.1 \text{ m}^2 \text{ g}^{-1}$ were obtained. A single curve has been drawn through these data points in Fig. 1-3.

We decided to study the dependence of the measured specific surface area on method of heat treatment, since our data for diesel exhaust particles and fly ash had demonstrated a marked change of specific surface area with outgassing temperature (Fig. 1-3). The data for aluminum oxide show an almost constant value over the temperature range 200°C - 450°C , as previously reported by Peri (Ref. 14). This, and the sample homogeneity make the material highly satisfactory as a surface area standard for the ^{85}Kr adsorption method. In contrast, the data for TiO_2 shows a measurable increase in specific surface area over the range 200°C - 450°C , so that the temperature of outgassing and the specific surface area of the sample must be specified if TiO_2 is used as a standard.

The data in Table 1-4 demonstrate both the agreement between the methods, and the intrinsic scatter in the data. In particular, these data demonstrate that the ^{85}Kr adsorption technique is free from major systematic error.

CONCLUSIONS

Each of the methods tested appears satisfactory, although each has different advantages. Where sufficient sample is available, the micro-balance appears to give the most reliable results, but this may reflect our greater experience in using this method. No systematic differences in data obtained by the three methods were noted, which implies that data obtained at laboratories using any one of these methods can be directly compared. Only the ^{85}Kr adsorption method provides simultaneously the ability to safely contain highly radioactive samples and to characterize reliably samples as small as ~ 2 mg in size. An illustration of the application of the method to samples of mixed U and Pu oxides is given in Part C.

REFERENCES

1. Rothenberg, S. J., "Coal Combustion Fly Ash Characterization: Adsorption of Nitrogen and Water," Atmos. Environ. **14**: 445, 1980.
2. Rothenberg, S. J. and Y. S. Cheng, "Coal Combustion Fly Ash Characterization: Rates of Adsorption and Desorption of Water," J. Phys. Chem. **84**: 1644, 1980.
3. Rothenberg, S. J., D. B. Kittleson, J. S. Dutcher, Y. Kiyoura and R. O. McClellan, "Adsorption of Xylene and Nitrogen by Diesel Exhaust Particulate," in A.C.S. 184th Meeting, Kansas City, September, 1982
4. Rothenberg, S. J., P. B. DeNee and P. Holloway, "Coal Combustion Fly Ash Characterization: Electron Spectroscopy For Chemical Analysis, Energy Dispersive X-Ray Analysis, and Scanning Electron Microscopy," Appl. Spectros. **34**: 549, 1980.
5. Eidson, A. F., P. B. DeNee and C. A. Macken, in Particle Analysis of Mixed Oxide Nuclear Fuel Materials, Colorado Springs, 1979.
6. DeNee, P. B. and R. L. Carpenter, "Elemental Analysis of Aerodynamically Separated Respirable Fly Ash Particles," Proceedings of the Society for Microbeam Analysis, 217, 1980.
7. Hock, J. L. and D. Lichtman, "Studies of Surface Layers on Single Particles of In-Stack Coal Fly Ash," Environ. Sci. Technol. **16**: 423, 1982.
8. Gregg, S. J. and K. S. W. Sing, "Adsorption, Surface Area and Porosity," Chapter 8, Academic Press, New York, 1967.
9. Nelson, F. M. and F. T. Eggertsen, "Determination of Surface Area Adsorption Measurements by a Continuous Flow Method," Anal. Chem. **30**: 1387, 1958.
10. Brunauer, S., P. H. Emmett and E. Teller, "Adsorption of Gases in Multi-Molecular Layers," J. Am. Chem. Soc. **60**: 309, 1938.
11. Karp, S., S. Lowell and Mustacciuolo, "Continuous Flow Measurement of Desorption Isotherms," Anal. Chem. **44**: 2395, 1972.
12. Rothenberg, S. J., P. B. Denee, Y. S. Cheng, R. L. Hanson, H. C. Yeh and A. F. Eidson, "Methods for the Measurement of Surface Areas of Aerosols by Adsorption," Adv. Colloid Interface Sci. **15**: 223, 1982.
13. Chenebault, P. and Schürenkamper, "The Measurement of Small Surface Areas by the B.E.T. Adsorption Method," J. Phys. Chem. **69**: 2300, 1965.
14. Peri, J. B., "Infrared and Gravimetric Study of the Surface Hydration of Gamma-Alumina," J. Phys. Chem. **69**: 211, 1965.

1. SURFACE AREA MEASUREMENTS

PART C. SPECIFIC SURFACE AREA DETERMINATIONS OF MIXED U AND Pu OXIDE PARTICULATES

Abstract — Specific surface area determinations were accomplished on samples of mixed U and Pu oxides using an ^{85}Kr adsorption technique. The particulate samples were obtained on filters during the inhalation exposure of animals to either $\text{UO}_2 + \text{PuO}_2$ treated at 750°C , $(\text{U,Pu})\text{O}_2$ treated at 1750°C , or "pure" PuO_2 treated at

850°C . Replicate determinations produced consistent results for two of the materials studied, with specific surface areas of $\sim 3 \text{ m}^2/\text{g}$ for one $(\text{U,Pu})\text{O}_2$ sample and $\sim 20 \text{ m}^2/\text{g}$ for "pure" PuO_2 . For two other materials, $\text{UO}_2 + \text{PuO}_2$ and one $(\text{U,Pu})\text{O}_2$ sample, the specific surface area increased for several determinations made successively on the same sample. Results of these determinations were used in determining the specific constant of solubility and these values used, in turn, in a simulation model of the retention, distribution and excretion of these particles following deposition in the lungs of animals.

PRINCIPAL INVESTIGATORS

J. A. Mewhinney
S. J. Rothenberg
A. F. Eidsann
G. J. Newton

The ^{85}Kr adsorption technique, described in Parts A and B of this paper, was used to determine the specific surface area of small samples (2-5 mg) of particles obtained during inhalation exposures of animals in studies designed to elucidate the retention, distribution and excretion of the inhaled material. In these studies, dogs, monkeys and rats were exposed to aerosols of either $\text{UO}_2 + \text{PuO}_2$ treated at 750°C , $(\text{U,Pu})\text{O}_2$ treated at 1750°C , or "pure" PuO_2 treated at 850°C . Analyses of tissue and excreted samples collected at selected times through 4 years after exposure includes separate analyses for Pu, Am, and U (where appropriate). To facilitate analyses and syntheses of these data sets, a biomathematical model was formulated to allow determination of differences and similarities. This model used the theory of Mercer (Ref. 1) on the role of dissolution of particulates deposited in lung to describe the rate of dissolution of Pu, Am, or U from these materials. The function describing dissolution is:

$$S(t) = F(\beta, \sigma_g) \quad (\text{Eq. 1-3})$$

where

$$\beta = \frac{\alpha_s k t}{\alpha_v D_m} \quad (\text{Eq. 1-4})$$

The surface shape factor, α_s , is the variable that can be determined using specific surface area measurements, k is the specific constant of solubility determined from in vitro solubility studies (Ref. 2), t is time, D_m is the mass median diameter calculated from the aerodynamic diameter measured by cascade impactor and α_v is the volume shape factor (set equal to unity). The ratio of the surface shape factor and the volume shape factor were calculated from the equation:

$$\frac{\alpha_s}{\alpha_v} = \frac{s/D^2}{m/\rho D^3} \quad (\text{Eq. 1-5})$$

where s is the surface area, D is the particle diameter, m is the mass and ρ is the density. Since $s = S_b m$ where S_b is the measured specific surface area in units of m^2/g the equation reduces to:

$$\frac{\alpha_s}{\alpha_v} = S_b D \quad (\text{Eq. 1-6})$$

METHODS AND MATERIALS

The particles used in the animal inhalation exposure were collected on membrane filters from the main exhaust vacuum manifold. For surface area determinations, small samples of the particles were transferred to the sample cell by brushing or carefully scraping material from the filter. These samples were attached to the vacuum manifold of the ^{85}Kr adsorption apparatus and the surface area was determined as described in Part A of this report. The samples were uniformly heated to 250°C for all determinations. Outgassing time was 16 hours for each sample run. The specific surface area of each sample was determined at least 3 times or until a consistent value was obtained, where possible.

Detailed procedures for sample handling, operation of the vacuum system and outgassing, and the quantification of ^{85}Kr adsorbed onto the particulates were presented in Part A of this paper.

RESULTS

The results of specific surface area determinations on several particulate samples of mixed U and Pu oxides and of PuO_2 are shown in Table 1-5.

DISCUSSION

The column labeled HEDL 1750 in Table 1-5 represents three replicate determinations on two different samples of particles collected at the Hanford Engineering and Development Laboratory (HEDL) during centerless grinding of $(\text{U,Pu})\text{O}_2$ fuel pellets. These pellets had been heat-treated at 1750°C for several hours prior to the finish grinding of the pellet to exact dimensions (Ref. 3). As can be noted from these data, the specific surface area measured for each sample did not change significantly with each repeat determination. The mean values of the two sets of three determinations did not differ significantly.

The sample of "pure" PuO_2 collected at the Babcock and Wilcox (B&W) mixed oxide fuel fabrication facility prior to mixing the PuO_2 and UO_2 powders also showed consistent results (Ref. 4, 5). The first 16-hour period of outgassing was accomplished without heating of the sample and resulted in a value near $9 \text{ m}^2/\text{g}$ whereas the second 16-hour period of outgassing, accomplished with heating at 250°C , produced a value two times greater in surface area ($\sim 19 \text{ m}^2/\text{g}$). Subsequently, two additional 16-hour outgassing runs with heating at 250°C produced values consistent with the second run (19 and $20 \text{ m}^2/\text{g}$). Heating the sample removes adsorbed water, but may also transform a sample, changing its composition or morphology, as previously reported for fly ash and diesel exhaust particles (Ref. 6, 7, 8). The consistent values obtained after successive 250°C outgassing show that the sample is stable at 250°C , as expected.

Both the electron microscopy and the density values previously reported (Ref. 3, 4, 5) had led to the conclusion that this sample was porous. The density data indicate a pore volume over 25%; samples whose pore volume exceeds 5% usually have specific surface areas greater than $5 \text{ m}^2/\text{g}$ (Ref 9). Thus, the high specific surface areas determined after outgassing at 25°C or 250°C are expected.

Particles deposited in lung have not been outgassed at all, and it might therefore appear that the data obtained after outgassing at room temperature were most relevant to a dissolution model. Surface sites on which moisture is adsorbed are not available for krypton or nitrogen adsorption (Ref. 7, 9). However, such sites are readily accessible for attack by the body fluids, since once a particle enters the lungs (100% relative humidity) most of the surface becomes covered by

Table 1-5. Specific Surface Area of Particulate Samples of Materials Used in Fabrication of U and Pu Mixed Oxide Nuclear Fuels

HEDL (U,Pu)O ₂ 1750°C		HEDL UO ₂ + PuO ₂ 750°C		B&W (U,Pu)O ₂ 1750°C		B&W "Pure PuO ₂ 850°C	
Specific		Specific		Specific		Specific	
Cumulative	Surface	Cumulative	Surface	Cumulative	Surface	Cumulative	Surface
Outgassing	Area	Outgassing	Area	Outgassing	Area	Outgassing	Area
Time (hr)	(m ² /g)	Time (hr)	(m ² /g)	Time (hr)	(m ² /g)	Time (hr)	(m ² /g)
16	2.78 ^a	16	2.82	16	3.76	16 ^b	8.98
32	2.90	32	3.35	32	8.44	32	19.1
48	2.66	48	4.79	48	15.9	48	19.0
Sample wt =	2.55 mg	64	5.82	64	20.9	64	20.3
		80	12.7	80	24.1	Sample wt =	1.99 mg
		Sample wt =	8.07 mg	96	28.3		
16	3.06 ^c			112	47.1		
32	3.08						
48	2.97			16 ^d	40.0		
Sample wt =	1.94 mg			Sample wt =	0.76 mg		

^aMean value \pm 1 SD = 2.78 ± 0.12

^bSample was not heated during initial outgassing period.

^cMean value \pm 1 SD = 3.04 ± 0.06

^dAfter 112 hours of outgassing, sample was returned to normal atmospheric pressure and room temperature for 10 day period, then rerun.

adsorbed water. Thus, the specific surface area obtained after removing adsorbed moisture ($19 \text{ m}^2 \text{ g}^{-1}$) appears more relevant to dissolution studies than that obtained when part of the surface is covered by adsorbed moisture.

Two samples, one collected at HEDL representing mechanically mixed powders of PuO₂ and UO₂ treated at 750°C and the second collected at B&W representing particulates produced by centerless grinding of (U,Pu)O₂ treated at 1750°C, show anomalous results. With each succeeding 16-hour outgassing period, the specific surface area determined increased substantially over the previous run. The HEDL 750°C sample determination was repeated five times for a total outgassing time of 80 hours and the B&W 1750°C sample was repeated seven times accumulating 112 hours of outgassing time. Neither of these samples showed any indication of approaching a consistent value. The B&W 1750°C sample was removed from the vacuum manifold and allowed to stand at room temperature and pressure for a period of 10 days before a replicate determination was made. Both Gregg and Sing (Ref. 9) and Füredi-Milhofer (Ref. 10) have reported that samples containing micro-pores may lose moisture from within these pores very slowly, taking days or weeks of heat treatment to attain a reproducible outgassed state. We have reported data on fly ash samples which required a minimum of 16 hours outgassing (Ref. 7). The density data for these samples previously reported by Newton, Stanley, Raabe (Ref. 3, 4, 5) demonstrate that the samples are porous. Thus, it appeared possible that the phenomenon observed was the result of the slow emptying of micro-pores, with consequent increase in surface available for adsorption of ⁸⁵Kr. The value obtained after ten days exposure to ambient air and a single night's outgassing demonstrated that some irreversible transformation occurred, since recontamination of the sample by moisture would have restored the

sample to its original state. The value determined after this interval was substantially greater than the original starting value (3.76 vs. 39.8 m²/g) and intermediate between the values determined after 96 and 112 hours of outgassing. To check on whether some systematic undetected deterioration of the equipment was causing the anomalous trend in values, each series of experiments was followed by a repeat determination of FAP surface area. As reported in Part A, within experimental error ($\pm 10\%$) no trend in the data for FAP was found. Table 1-3, Part A, shows data for two such experiments, similar self-consistent data were found in all cases. Thus, the trend reported for these samples appears to be real, rather than an instrumental artifact.

The cause of the increased specific surface area measured in these latter two particle samples is not known. It seems obvious that a transformation was taking place, perhaps due to micropore formation during heating and outgassing. Schaner, (Ref. 11) in a metallographic study of UO₂/U₄O₉ phase diagram, observed that prolonged annealing caused separation of the denser U₄O₉ from the UO_{2+x}, with voids (or pores) formed at the grain boundary. Phase transformations caused by annealing might explain the systematic change in sample properties with outgassing (annealing) time. However, this response was not observed for the (U,Pu)O₂ particulates collected at HEDL which had identical physical chemical characteristics and thermal history.

For purposes of applying these specific surface area determinations for use in the biomathematical model, values for three materials pertinent to the animal studies were taken as; 1) for UO₂ + PuO₂ particulates as the mean of the first two determinations (3.1 m²/g), 2) for (U,Pu)O₂ the mean of the six determinations on two separate samples (2.9 m²/g) and 3) for "pure" PuO₂ the mean of the three replicate runs where heating at 250°C was accomplished (19.5 m²/g). The calculation of the surface shape factor using Equation 1-6 results in α_s values of 19.3, 22.0 and 108.0 for the UO₂ + PuO₂ treated at 750°C, (U,Pu)O₂ treated at 1750°C, and the "pure" PuO₂ treated at 850°C. The results of the use of these values in the biomathematical model are detailed on pp. 21 to 32 of this report.

REFERENCES

1. Mercer, T. T., "On the Role of Particle Size in the Dissolution of Lung Burdens," Health Phys. 13: 1211-1221, 1967.
2. Eidson, A. F. and J. A. Mewhinney, "In Vitro Dissolution of Respirable Aerosols of Industrial Uranium and Plutonium Mixed-Oxide Nuclear Fuels," U. S. Nuclear Regulatory Commission Report, NUREG/CR-2171, LMF-79, 1981*.
3. Raabe, O. G., G. J. Newton, C. J. Wilkinson and S. V. Teague, "Plutonium Aerosol Characterization Inside Safety Enclosures at a Demonstration Mixed-Oxide Fuel Fabrication Facility," Health Phys. V35: 649-661, ____.
4. Newton, G. J., "Mixed Oxide Fuel Fabrication," in Radiation Exposure and Risk Estimates for Inhaled Airborne Radioactive Pollutants Including Hot Particles - Annual Report for Period July 1, 1976 - June 30, 1977, NUREG/CR-0010, 1978*.
5. Stanley, J. A. and G. J. Newton, "Further Sampling of Aerosolized Mixed Oxide Nuclear Fuel in a Fabrication Facility," in Radiation Dose Estimates and Hazard Evaluation for Inhaled Airborne Radionuclides - Annual Report for Period July 1, 1977 to June 30, 1978, NUREG/CR-0673, LMF-63, 1979*.

6. Hill, J. O., S. J. Rothenberg, G. M. Kanapilly, R. L. Hanson and B. R. Scott, "Activation of Immune Complement by Fly Ash Particles From Coal Combustion," Environ. Res. 28: 113-122, 1982.
7. Rothenberg, S. J. "Coal Combustion Fly Ash Characterization: Adsorption of Nitrogen and Water," Atmos. Environ. 14: 445-456, 1980.
8. Rothenberg, S. J., D. B. Kittleson, J. S. Dutcher, R. Kiyora and R. O. McClellan, "Adsorption of Xylene and Nitrogen by Diesel Exhaust Particulates," Paper 54, Colloid Division, 184th ACS National Meeting, Kansas, Sept. 12th-17th, 1982.
9. Gregg, S. J. and K. S. W. Sing, "Adsorption, Surface Area and Porosity," Academic Press, New York, 1967.
10. Füredi-Milhofer, V., Hlady, F. S. Baker, R. A. Beebe, N. W. Wikholm and J. S. Kittelberger, "Temperature-Programmed Dehydration of Hydroxyapatite," J. Colloid Interface Sci. 70: 1-9, 1979.
11. Schaner, B. E., "Metallographic Determination of the UO_2 - U_4O_9 Phase Diagram," J. Nuclear Materials 2,2: 110-120, 1980.

*Available for purchase from the NRC/GPO Sales Program, U. S. Nuclear Regulatory Commission, Washington, DC 20555 or from the National Technical Information Services, Springfield, VA 22161.

2. MODELS OF RETENTION, DISTRIBUTION AND EXCRETION OF PU, AM AND U
BY BEAGLE DOGS, CYNOMOLGUS MONKEYS AND FISCHER-344 RATS
FOLLOWING INHALATION OF INDUSTRIAL AEROSOLS

Abstract — Beagle dogs, Cynomolgus monkeys and Fischer-344 rats received inhalation exposure to one of three aerosols derived from industrial production of mixed U, Pu oxide nuclear fuels. Sacrifice of 2 dogs, 1 monkey and 5 rats at times up to 4 years after inhalation resulted in information on lung

PRINCIPAL INVESTIGATORS

J. A. Mewhinney

A. F. Eidson

retention, tissue distribution and modes of excretion. Biomathematical models have been formulated to synthesize these data sets for each element of interest; Pu, Am and U. Physical chemical characterization of the aerosols allowed use in the models of an equation to describe the rate of dissolution of particles deposited in lung. Results of these efforts indicate that for a given element, slight differences in the retention, distribution and excretion of that element for a given species can be accounted for by the differences in the physical chemical characteristics of the aerosol. For a given aerosol, significant differences in retention, distribution and excretion were found among the three animal species. Also, for each species, differences were found in the retention, distribution and excretion of the elements of Pu, Am and for U (when present) for each aerosol.

Three radiation dose distribution studies have been conducted to provide information regarding the biological fate, associated distribution of radiation dose to tissue, and the implications for potential health consequences of an inhalation exposure involving nuclear fuel materials. Three different materials were studied using the same experimental protocol. In each study, Beagle dogs, Cynomolgus monkeys and Fischer-344 rats were exposed by inhalation to one of three aerosols: 750°C treated $UO_2 + PuO_2$, 1750°C treated $(U,Pu)O_2$ or 850°C treated "pure" PuO_2 . Lung retention, tissue distribution and mode of excretion of $^{238-240}Pu$, ^{241}Am and U (where present) have been quantified by analysis of tissue and excreta samples from animals sacrificed at selected times through four years after inhalation exposure.

To synthesize these data, biomathematical models have been formulated to provide good descriptions of each data set. A fundamental precept of the modeling process was to use common rate constants wherever possible for each element and species for each aerosol thus providing a structure within which to compare and contrast data from these studies. To simplify these comparisons, subsequent sections of this report will be sub-divided into parts based on the element being quantified.

METHODS

The inhalation exposure procedures and the physical chemical characteristics of the three aerosols have been described (Ref. 1, 2) as has the in vitro solubility of Pu, Am and U in these materials in several solvents (Ref. 3). A preliminary report regarding the model applied to Pu retention, distribution and excretion in dogs exposed to those aerosols has been presented (Ref. 4).

The models formulated to describe the retention, distribution and excretion of Pu, Am and U (where appropriate) contained in these aerosols use, in common, the mathematical expression derived by Mercer (Ref. 5) for description of the process of dissolution of particulates deposited

in lung. Specifically, dissolution is described as a function of the physical chemical characteristics of the deposited particles as given in the following equations:

$$S(t) = F(\beta, \sigma_g) \quad (\text{Eq. 2-1})$$

and

$$\beta = \frac{\alpha_s k t}{\sigma_g \rho D_m} \quad (\text{Eq. 2-2})$$

where σ_g is the geometric standard deviation of the aerosol size distribution, α_s is the surface shape factor, k is the dissolution rate of the element of interest for the particle, ρ is the density of the particle, D_m is the mean geometric diameter of the particle and α_v is the volume shape factor.

The model used to describe the data sets from these studies was adapted from a model found useful in describing similar data from a study in which dogs were exposed by inhalation to aerosols of $^{241}\text{AmO}_2$ (Ref. 6).

As a starting point in the modeling of Pu retention, distribution and excretion in the dogs for these studies, all rate constants for internal organ compartments which communicate with the blood compartment were set identical to the rate constants used in a model of ^{238}Pu retention, distribution and excretion over a four-year period following inhalation of $^{238}\text{PuO}_2$ by dogs (Ref. 7). Similarly, for modeling of Am in these studies, these same rate constants were set equal to values from the model of ^{241}Am retention, distribution and excretion following inhalation of $^{241}\text{AmO}_2$ by dogs (Ref. 6).

Mucociliary clearance of these materials from lung is described in the model using;

$$M(t) = b_1 e^{-\lambda_1 t} + b_2 e^{-\lambda_2 t} + b_3 \quad (\text{Eq. 2-3})$$

where b_i and λ_i are empirically determined in the iterative fitting process. The values used for variables in the equations which describe solubilization of Pu, Am or U from the aerosols (Eq. 2-1, 2-2) used in these studies were calculated from physical chemical characterization information determined from several types of measurements made on samples of the aerosol obtained during animal inhalation exposures. The geometric diameter (D_m) and geometric standard deviation (σ_g) of the aerosols were determined from data obtained by cascade impactor. Density (ρ) was determined from x-ray diffraction measurements of the crystal lattice unit cell dimension. Surface shape factor (α_s) was determined as given separately in this report (pp. 16 to 20). The constant of solubility (k) was determined from in vitro solubility studies (Ref. 3) conducted on aerosol samples using a synthetic serum ultrafiltrate (SUF).

One departure from techniques used previously in the models of $^{241}\text{AmO}_2$ and $^{238}\text{PuO}_2$ retention, distribution and excretion cited above was the insertion in these models of a small fraction of the initial lung burden of the element of interest directly into the blood compartment at time zero in the simulation. These fractions, listed in Table 2-1, represent those fractions of the aerosol which undergo very rapid dissolution with halftimes of less than 2.2 days (Ref. 3). These rapid dissolution fractions are in contrast with the majority fraction of these elements which exhibit dissolution halftimes of several hundred to thousands of days.

The model was implemented using a simulation language, GASP IV, programmed in FORTRAN IV (Ref. 8) on a PDP VAX/780 computer. The simulations were run iteratively and the results plotted to judge conformance with the data.

RESULTS

Plutonium. A schematic diagram of the model with the rate constants derived for the retention, distribution and excretion of Pu for the dog, monkey and rat is shown in Figure 2-1. Where a particular rate constant differs among the three species, the appropriate values are suffixed with

Table 2-1. Measured Values for Variable in Equation Describing Solubilization of Particles Deposited in Lungs of Dogs, Monkeys and Rats.

Radio-nuclide	Species	Aerosol	Density (g/cm ³)	Particle Diameter (x10 ⁻⁴ cm)	Geometric Standard Deviation	Specific Constant of Solubility (g/cm ² /day)	Surface Shape Factor	F ^a
Plutonium	Dog	UO ₂ + PuO ₂	11.5	0.59	1.8	1.3 x 10 ⁻¹⁰	19.3	0.4
		(U,Pu)O ₂	11.5	0.66	1.8	7.1 x 10 ⁻¹⁰	22.0	4.6
		"pure" PuO ₂	11.5	0.47	1.7	1.5 x 10 ⁻¹⁰	108	0.1
	Monkey	UO ₂ + PuO ₂	11.5	0.34	1.6	8.1 x 10 ⁻¹⁰	19.3	0.4
		(U,Pu)O ₂	11.5	0.61	1.7	6.6 x 10 ⁻¹⁰	22.0	4.6
		"pure" PuO ₂	11.5	0.56	1.8	1.8 x 10 ⁻¹⁰	108	0.1
	Rat	UO ₂ + PuO ₂	11.5	0.59	1.8	1.4 x 10 ⁻⁹	19.3	0.4
		(U,Pu)O ₂	11.5	0.59	1.7	6.4 x 10 ⁻¹⁰	22.0	4.6
		"pure" PuO ₂	11.5	0.56	2.0	1.8 x 10 ⁻¹⁰	108	0.1
Americium	Dog	UO ₂ + PuO ₂	11.5	0.59	1.8	9.7 x 10 ⁻⁹	19.3	2.0
		(U,Pu)O ₂	11.5	0.66	1.8	2.5 x 10 ⁻⁹	22.0	6.7
		"pure" PuO ₂	11.5	0.47	1.7	5.1 x 10 ⁻¹⁰	108	0.1
	Monkey	UO ₂ + PuO ₂	11.5	0.34	1.6	6.1 x 10 ⁻¹⁰	19.3	2.0
		(U,Pu)O ₂	11.5	0.61	1.7	2.3 x 10 ⁻⁹	22.0	6.7
		"pure" PuO ₂	11.5	0.56	1.6	6.0 x 10 ⁻¹⁰	108	0.1
	Rat	UO ₂ + PuO ₂	11.5	0.59	1.8	1.1 x 10 ⁻⁹	19.3	2.0
		(U,Pu)O ₂	11.5	0.59	1.7	2.2 x 10 ⁻⁹	22.0	6.7
		"pure" PuO ₂	11.5	0.56	2.0	6.0 x 10 ⁻¹⁰	108	0.1
Uranium	Dog	UO ₂ + PuO ₂	11.5	0.59	1.8	4.8 x 10 ⁻⁸	19.3	37.
		(U,Pu)O ₂	11.5	0.66	1.8	1.9 x 10 ⁻⁹	22.0	26.
	Monkey	UO ₂ + PuO ₂	11.5	0.34	1.6	3.0 x 10 ⁻⁸	19.3	37.
		(U,Pu)O ₂	11.5	0.61	1.7	1.7 x 10 ⁻⁹	22.0	26.
	Rat	UO ₂ + PuO ₂						
		(U,Pu)O ₂						

^aF=Percentage of initial lung burden dissolving with halftimes less than ~ 2 days

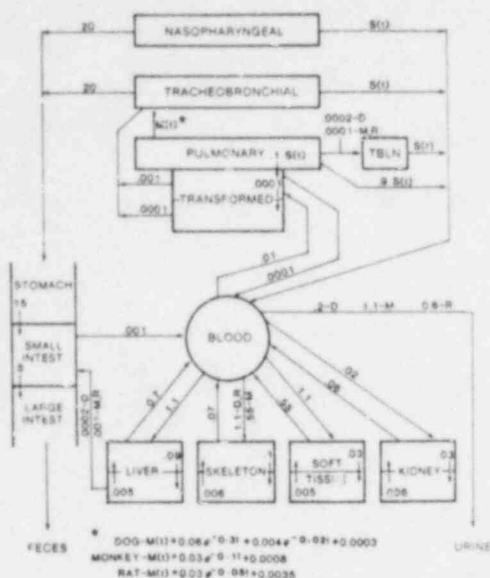


Figure 2-1. Schematic diagram of the biomathematical model used to describe the retention, distribution and excretion of Pu in dogs, monkeys and rats following inhalation of either $\text{UO}_2 + \text{PuO}_2$, $(\text{U,Pu})\text{O}_2$ or "pure" PuO_2 . Where more than one rate constant is shown for a given pathway, the suffix letter D (dogs), M (monkeys) and R (rats) indicates which constant is associated with each species.

D for dog, M for monkey and R for rat. The rate constants shown in each case apply to all three aerosol forms, i.e. $\text{UO}_2 + \text{PuO}_2$, $(\text{U,Pu})\text{O}_2$ and PuO_2 , in each animal species. Table 2-1 lists the values for variables in the equations (Equations 2-1, 2-2) used to describe solubilization of Pu from the three aerosol forms for each species. The adequacy of the model description of these data sets may be judged from Figures 2-2 (dog), 2-3 (monkey) and 2-4 (rat). In these latter three figures the data points represent individual animals and the curves represent the model description.

Americium. The schematic diagram with the appropriate rate constants derived for the retention, distribution and excretion of Am for the dog, monkey and rat are shown in Figures 2-5. As was the case for Pu, these rate constants for Am apply to all three aerosol forms for each species. Table 2-1 lists the values for variables in the equations (Equations 2-1, 2-2) used to describe solubilization of Am for the three aerosol forms for each species. The adequacy of the model descriptions of these data may be judged from Figures 2-6 (dog), 2-7 (monkey) and 2-8 (rat).

Uranium. As discussed previously for Pu and Am the schematic diagram with appropriate rate constants derived for retention, distribution and excretion of U for the dog and monkey is shown in Figure 2-9. In this case, these constants apply for the $\text{UO}_2 + \text{PuO}_2$ and the $(\text{U,Pu})\text{O}_2$ aerosols. Table 2-1 lists the values for variables in Equations 2-1, 2-2 for the two aerosols containing uranium for each species. The adequacy of the descriptions of these data may be judged from Figures 2-10 (dogs) and 2-11 (monkeys).

DISCUSSION

The biomathematical model adapted from previous work at this Institute was found to be applicable to these data sets. A single departure from previous uses was the insertion of a small fraction of the initial lung burden into the blood compartment at zero time in the simulation. This was done in recognition of situations found for several laboratory-produced actinide oxide aerosol materials, as well as these industrially derived aerosols, wherein a small fraction of the deposited material dissolves quite rapidly with half-time of about 2 days. This phenomenon has been documented from *in vitro* solubility studies (Ref. 3).

Self-imposed constraints in application of the model simulation procedure included use of a single mechanical-clearance function $M(t)$ for each species and each aerosol without regard to the

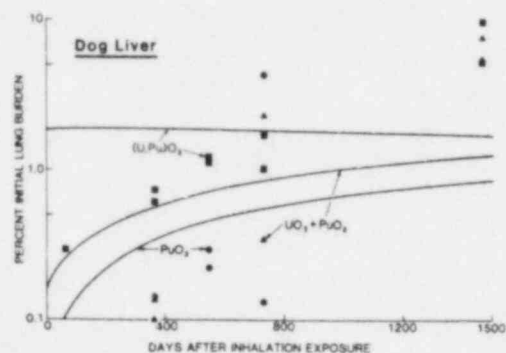
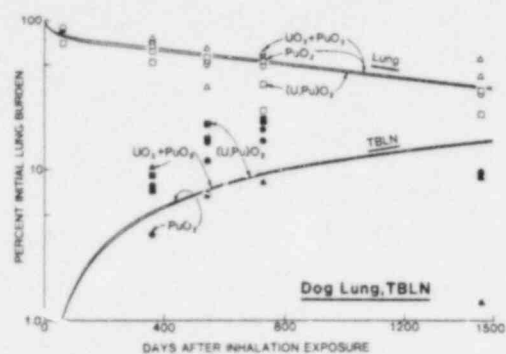


Figure 2-2. Lung retention, tracheobronchial lymph node and liver uptake and retention of Pu in dogs following inhalation of either $UO_2 + PuO_2$, $(U,Pu)O_2$ or "pure" PuO_2 . Data points represent individual dogs whereas curves represent model predictions.

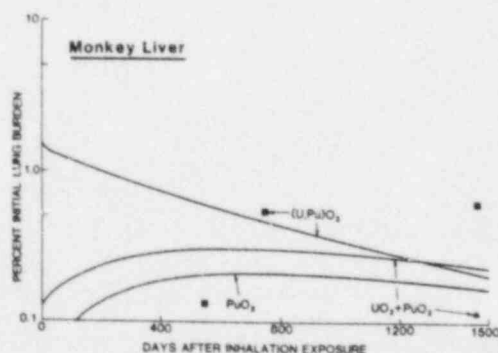
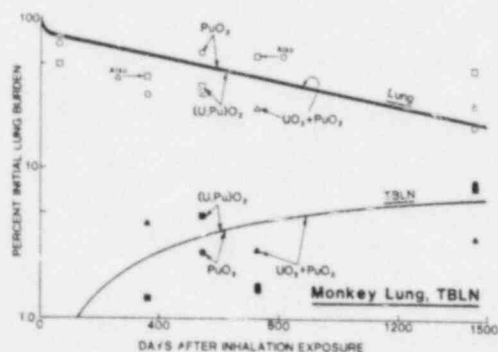


Figure 2-3. Lung retention, tracheobronchial lymph node and liver uptake and retention of Pu in monkeys following inhalation of either $UO_2 + PuO_2$, $(U,Pu)O_2$ or "pure" PuO_2 . Data points represent individual monkeys whereas curves represent model predictions.

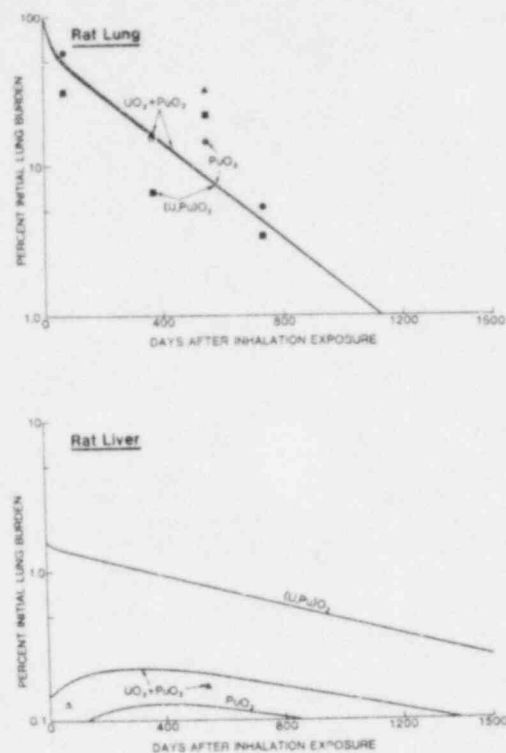


Figure 2-4. Lung retention, tracheobronchial lymph node and liver uptake and retention of Pu in rats following inhalation of either $UO_2 + PuO_2$, $(U,Pu)O_2$ or "pure" PuO_2 . Data points represent individual rats whereas curves represent model predictions.

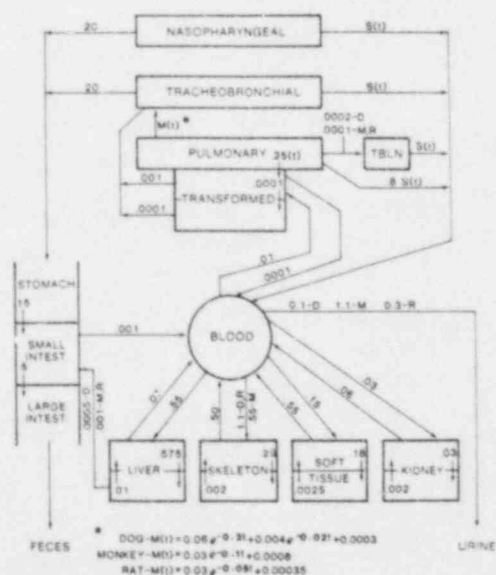


Figure 2-5. Schematic diagram of the biophysical model used to describe the retention, distribution and excretion of Am in dogs, monkeys and rats following inhalation of either $UO_2 + PuO_2$, $(U,Pu)O_2$ or "pure" PuO_2 . Where more than one rate constant is shown for a given pathway, the suffix letter D (dogs), M (monkeys) and R (rats) indicates which constant is associated with each species.

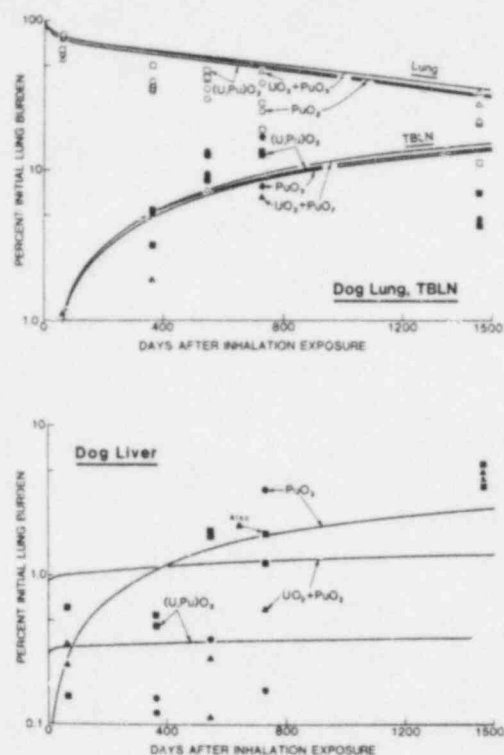


Figure 2-6. Lung retention, tracheobronchial lymph node and liver uptake and retention of Am in dogs following inhalation of either $UO_2 + PuO_2$, $(U,Pu)O_2$ or "pure" PuO_2 . Data points represent individual dogs whereas curves represent model predictions.

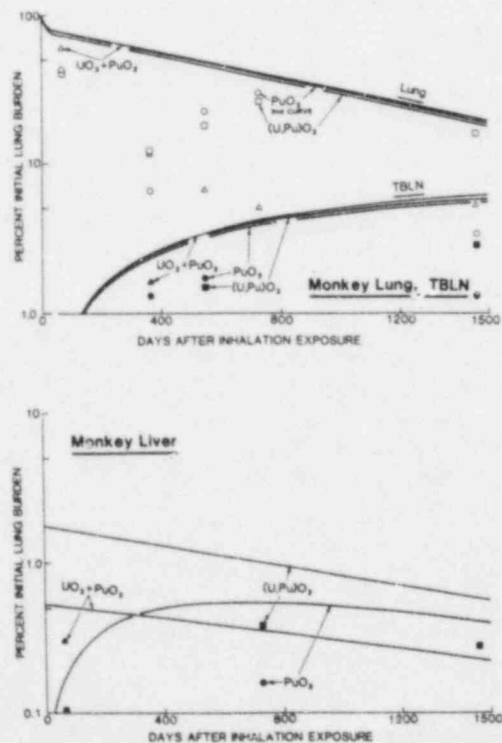


Figure 2-7. Lung retention, tracheobronchial lymph node and liver uptake and retention of Am in monkeys following inhalation of either $UO_2 + PuO_2$, $(U,Pu)O_2$ or "pure" PuO_2 . Data points represent individual monkeys whereas curves represent model predictions.

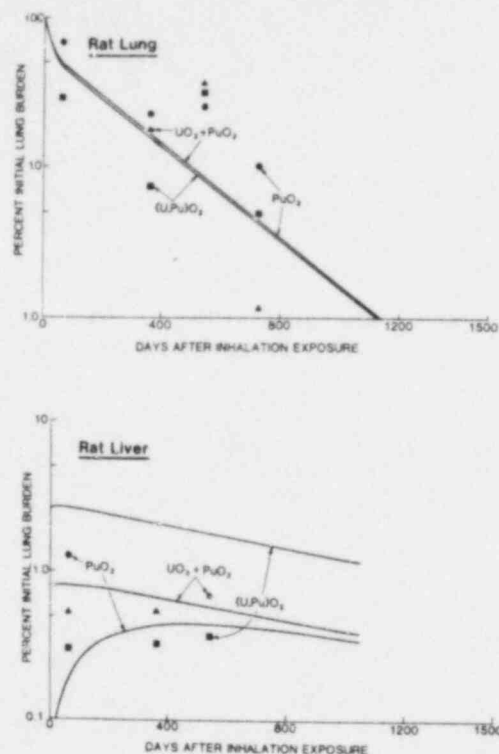


Figure 2-8. Lung retention, tracheobronchial lymph node and liver uptake and retention of Am in rats following inhalation of either $UO_2 + PuO_2$, $(U,Pu)O_2$ or "pure" PuO_2 . Data points represent individual rats whereas curves represent model predictions.

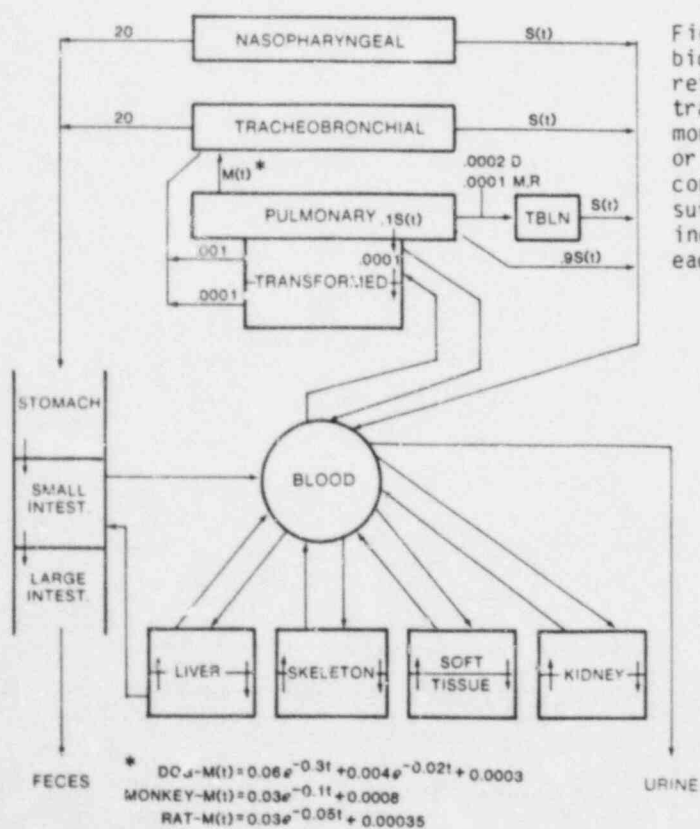


Figure 2-9. Schematic Diagram of the biomathematical model used to describe lung retention and uptake and retention in the tracheobronchial lymph nodes of U in dogs and monkeys following inhalation of $NO_2 + PuO_2$ or $(U, Pu)O_2$. Where more than one rate constant is shown for a given pathway the suffix letter D (dogs) and M (monkeys) indicates which constant is associated with each species.

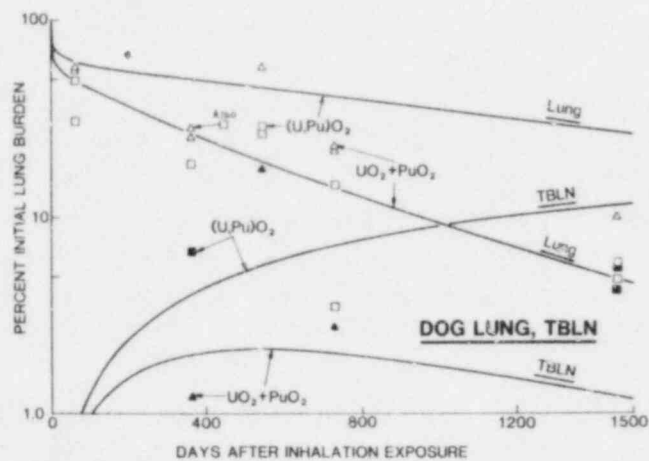


Figure 2-10. Lung retention and tracheobronchial lymph node uptake and retention of U in dogs following inhalation of either $UO_2 + PuO_2$ or $(U, Pu)O_2$. Data points represent individual dogs whereas curves present model predictions.

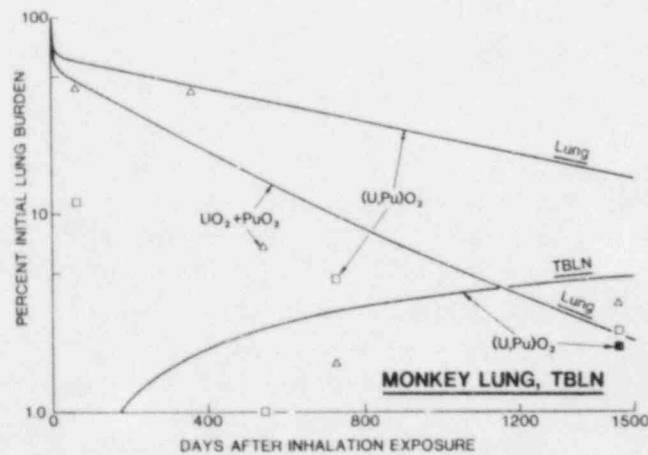


Figure 2-11. Lung retention and tracheobronchial lymph node uptake and retention of U in monkeys following inhalation of either $UO_2 + PuO_2$ or $(U, Pu)O_2$. Data points represent individual monkeys whereas curves present model predictions.

individual element under study. This constraint is consistent with the premise that the elemental components of these particulate materials are intimately associated in each single particle. A second constraint was to modify only those rate constants in the model which deal with solubilized material (i.e., ionic form) as it relates to distribution and excretion of the given element.

While complete data were available from these studies on Pu and Am in all tissues of each species, the data for U are incomplete. Due to relatively high natural U content in tissues and excreta of rats, only data for lung retention and tracheobronchial lymph node uptake and retention of U are presented for dogs and monkeys.

Plutonium. The agreement between model generated curves and the lung retention, tracheobronchial lymph node and liver uptake and retention data for dogs are quite good (Fig. 2-2). Only slight differences in lung retention of Pu were noted among the three aerosol forms. These differences appear to be related entirely to small changes in the variables in the solubility function. A large difference in specific surface area was measured for the "pure" PuO_2 aerosol resulting in a surface shape factor approximately 5 times greater than for the two mixed oxide aerosols. Even in this case the much larger surface area does not predict significantly more Pu being dissolved due to the inherently low dissolution rate for PuO_2 .

This model of Pu retention, distribution and excretion was tested on the results of a study underway at this Institute in which dogs are sacrificed at selected intervals after inhalation exposures to laboratory-produced aerosols of $^{239}\text{PuO}_2$ (Ref. 9). Good agreement between the data from that study and model generated curves were apparent.

The model predictions of lung retention, tracheobronchial lymph node and liver uptake and retention of Pu for monkeys following inhalation of each of the three aerosols may be judged from Figure 2-3 as showing quite good agreement with the data. Only a few changes in rate constants were necessary to convert the dog Pu model to provide good descriptions of the monkey data (see Fig. 2-1). The time varying mechanical clearance rate, $M(t)$, was altered to provide adequate description of the fecal excretion of Pu from monkey. The rate constant describing the rate of transfer from the second liver subcompartment to the small intestine was increased as was the rate constant describing urinary excretion of Pu from the blood compartment. The rate constant describing intake of Pu from blood to skeleton was reduced for monkeys.

For modeling of Pu retention, distribution and excretion in rats, the dog model was again modified. The results of these modifications provide good agreement between the model generated curves and the data for rats (Fig. 2-6). The changes necessary to adapt the model to rats include changes in the time varying rate of mechanical clearance, the rate for transfer from the second subcompartment of liver to small intestine and the rate of urinary excretion (see Fig. 2-1).

The results of these efforts indicate that when the Pu component of the three aerosols is compared for any one of the three species slight differences in the Pu retention, distribution and excretion can be ascribed to the known differences in the physical chemical characteristics of the aerosol. This may be related to the relatively insoluble nature of all the particles. Thus, even though the surface shape factor is a factor of 5 times larger for the "pure" Pu particles compared to either of the mixed U and Pu oxides, the inherently low solubility of the Pu component does not allow expression of this difference.

A different type of conclusion is valid when comparisons are made of the role of animal species in determining retention, distribution and excretion of the Pu component of the three aerosols. The differences in retention, distribution and excretion observed in comparison of raw data from these studies are highlighted when the model simulations are accomplished. To achieve good agreement between the model generated curves and the data for each species selected rate constants must be adjusted. As noted above, these adjustments included rates of mechanical clearance, urinary excretion, uptake to skeleton and rates of loss from liver via the biliary

route. Thus, lung retention halftimes for the Pu component from the aerosols is species dependent and is largely controlled by different rates of mechanical clearance. These differences are in accord with observations previously reported for dogs and rats for several inhaled, relatively insoluble materials (Ref. 9-10). Differences among these three species for liver retention of alpha emitting radioactive materials have also been previously reported (Ref. 9-10).

Americium. The modeling of retention, distribution and excretion of the Am component of these aerosols in each species proceeded by the same methods as for Pu. A self-imposed restriction for modeling the Am component was to use the identical expressions for the time-varying rate of mechanical clearance for each species as had been found satisfactory for the Pu component. This restriction was imposed simply due to the fact that the Am present was due to decay of ^{241}Pu present in the particles rather than the presence of separate particles of AmO_2 . Just as for Pu, the rate constants for all compartments communicating with blood were taken from an identical model used in describing the retention, distribution and excretion of ^{241}Am following inhalation of $^{241}\text{AmO}_2$ (Ref. 6).

The simulation modeling accomplished for the Am component of these aerosols did not result in completely satisfactory description of the data for the three species. In all cases the model slightly overpredicts lung retention. Repeated attempts to improve the description of lung retention were unsuccessful within the constraint mentioned above and of total materials balance. In depth analyses of the cause for this discrepancy indicated that it may be related to a phenomenon of early, relatively rapid, dissolution of Am present on the surface of particles followed by much slower dissolution of Am from particles as the predominant elemental composition and chemical form of the particle matrix dissolves at a slower rate. This is a consistent explanation that is supported by the *in vitro* solubility studies (Ref. 3) which show that at times greater than a few days after immersion in solvent the Am component of the particulates dissolves much slower ($k \geq \sim 1 \times 10^{-9}$) than for $^{241}\text{AmO}_2$ particles ($k = 1.5 \times 10^{-6}$).

As can be seen in Figures 2-6, 2-7 and 2-8 the lung retention is overestimated. However, tissue distribution and excretion rates are relatively well described. Thus, while the Am model did not provide completely adequate descriptions the fact that the Am content of these particulates is relatively small, and contribute relatively small increments of radiation dose to tissue, use of these predictions would lead to only a slight over-estimate of total radiation dose to lung.

Uranium. The lung retention of U for dogs and monkey exposed to the $\text{UO}_2 + \text{PuO}_2$ and the $(\text{U}, \text{Pu})\text{O}_2$ aerosols was modeled using the same time varying rate of mechanical clearance $M(t)$ as was used for the Pu and Am components of these materials for these two species. As may be seen in Figure 2-10 (dogs) and Figure 2-11 (monkeys), the model prediction for the $\text{UO}_2 + \text{PuO}_2$ aerosol agrees with the data. For the $(\text{U}, \text{Pu})\text{O}_2$ aerosol, however, lung retention is overestimated substantially by the model. It appears that the U component of the $(\text{U}, \text{Pu})\text{O}_2$ aerosol is more soluble in dogs and monkeys than would be expected from *in vitro* solubility studies using the SUF solvent. This is in contradiction to the results for the Pu and Am components of this aerosol.

CONCLUSIONS

The results of these modeling efforts indicate that the Pu component of these materials can be adequately described using the theory of Mercer to describe the rate of dissolution. Physical chemical determinations of specific surface area, density, particle size and size distribution and the rate of dissolution of the particulates were used in the equations of Mercer to show that for a single species of animal, the lung retention of the Pu component was not different for the three aerosols studied.

Specific differences in lung retention, tissue distribution and rates of excretion were discernable among the three animal species for each aerosol. These differences were attributable to differing rates of mechanical clearance, rate of transfer of Pu from liver to the gastrointestinal tract via the biliary route and the fraction of Pu in the blood compartment excreted rapidly through the kidney to urine.

REFERENCES

1. Eidson, A. F., "Generation of Aerosols of Mixed Uranium-Plutonium Oxides from Dry Powders for Animal Inhalation Exposures," in Radiation Exposure and Risk Estimates for Inhaled Airborne Radioactive Pollutants Including Hot Particles - Annual Report for Period 1 July 1976 to 30 June 1977, NUREG/CR-0010, 1978.*
2. Eidson, A. F., "Physical Chemical Analysis of Industrial Mixed Uranium, Plutonium Oxide Fuels," in Radiation Exposure and Risk Estimates for Inhaled Airborne Radioactive Pollutants Including Hot Particles - Annual Report for Period 1 July 1977 to 30 June 1978, NUREG/CR-0673, 1979.*
3. Eidson, A. F. and J. A. Mewhinney, "In Vitro Dissolution of Respirable Aerosols of Industrial Uranium and Plutonium Mixed-Oxide Nuclear Fuels," U.S. Nuclear Regulatory Commission Report, NUREG/CR-2171, LMF-79, 1981.*
4. Mewhinney, J. A., A. F. Eidson, J. A. Stanley and R. A. Guilmette, "Radiation Dose Patterns in Rats, Dogs and Monkeys Following Inhalation of Industrial Aerosols Formed in Fabrication of Mixed Oxide Nuclear Fuel," in Radiation Dose Estimate and Hazard Evaluations for Airborne Radionuclides - Annual Report for Period July 1980 to June 1981, NUREG/CR-2512, 1981.*
5. Mercer, T. T., "On the Role of Particle Size in the Dissolution of Lung Burdens," Health Phys. 13: 1211-1221, 1967.
6. Mewhinney, J. A. and W. C. Griffith, "Models of Am Metabolism in Beagles and Humans," Health Phys. 42: 629-644, 1982.
7. Mewhinney, J. A. and J. H. Diel, "Retention of Inhaled ^{238}PuO in Beagles: A Mechanistic Approach to Description," Health Phys. (in press) 1983.
8. Pritsker, A. A. B., The GASP IV Simulation Language, New York, Wiley and Sons, 1974.
9. Bair, W. J., J. E. Ballou, J. F. Park and C. L. Sanders, "Plutonium in Soft Tissue with Emphasis on the Respiratory Tract", in Uranium, Plutonium and the Transplutonic elements, Handbook of Experimental Pharmacology, Springer-Verlag, New York, 1973.
10. Durbin, P. W. "Metabolism and Biological Effects of the Transplutonium Elements" in Uranium, Plutonium and the Transplutonium Elements, Handbook of Experimental Pharmacology, Springer-Verlag, New York, 1973.

*Available for purchase from the NRC/GPO Sales Program, U.S. Nuclear Regulatory Commission, Washington, DC 20555 and/or from the National Technical Information Services, Springfield, VA 22161

3. BIOLOGIC EFFECTS IN RATS, BEAGLE DOGS AND MONKEYS AFTER INHALATION OF INDUSTRIAL MIXED OXIDES OR PuO_2

Abstract — Rats, dogs and monkeys were exposed, nose-only, to aerosols of mixed oxides of U and Pu or "pure" PuO_2 from nuclear fuel fabrication facilities. In animals held for long periods, biologic effects were noted. Lung tumors were induced in both rats and dogs with doses to lung ranging from 190 to 16,000 rads in rats and 2,500-4,800 rads in dogs. None of the 3 monkeys held for long-term study and sacrificed four years after exposure developed tumors with lung doses ranging from 2,870 to 4,720 rads.

PRINCIPAL INVESTIGATORS

F. F. Hahn

J. A. Mewhinney

The purpose of this project does not primarily involve study of the biologic effects due to absorbed radiation dose. Such effects however, have been observed in animals that died during the holding period for study of long-term radionuclide retention and distribution patterns. The observation and reporting of these effects is an important link between studies done using laboratory-produced aerosols and studies using aerosols as actually found in nuclear fuel facilities. It also allows the comparison of responses among different species.

METHODS

Methods used to obtain initial lung burden values and lung retention functions for these studies have been previously reported (Ref. 1, 2). The retention information and initial lung burdens used for dose calculations have been updated from these reports.

Radiation dose in rads was calculated from the equation:

$$\text{cumulative dose (rads)} = \frac{51.2 \bar{E} f g A}{W} \int_0^t B(t) dt \quad (\text{Eq. 3-1})$$

where: 51.2 = conversion factor, \bar{E} = energy per disintegration in MEV, f = absorbed fraction of energy, g = fractional yield of emission, A = initial lung burden in μCi , W = lung weight in grams, $B(t)$ = lung retention expressed as a fraction of the initial lung burden as a function of time after inhalation exposures. The dose to lung was calculated separately for Am and Pu and the two values summed to arrive at total dose to lung for each animal that died. Results of the calculations are shown in Table 3-1 for rats, Table 3-2 for dogs and Table 3-3 for monkeys where sufficient data are available.

Animals that died or were euthanized were given detailed postmortem examinations that included observation of all organ systems. Tissue sections of all major organs and grossly visible lesions were made for histologic evaluation. Sections were routinely stained with hematoxylin and eosin.

RESULTS AND DISCUSSION

A large number of rats died with lung tumors (Table 3-1). Two general morphologic types of primary lung tumors were found in the rats, adenocarcinoma and squamous cell tumors. The adenocarcinomas were characterized by large, anaplastic, cuboidal cells with basilar nuclei which formed small tubular or acinar structures. In some tumors, the acini were occasionally lined by keratinized squamous epithelium giving an adeno-squamous appearance. Some tumors had foci that were papillary, or mucinous in nature or were solid sheets of anaplastic cells. In some cases,

Table 3-1. Rats Exposed to Mixed-Oxide Aerosols that Died Before Scheduled Sacrifice Times

Animal Number	Exposure Aerosol	Survival (DPE) ^b	ILB ^a (nCi)	Cumulative Lung Dose To Death (rads)	Significant Lesions
1933 20	UO ₂ + PuO ₂ ^c + Binder	491	180	10,000	Squamous cell carcinoma, squamous cell papilloma, lung
1933 21	"	453	130	5,800	Squamous cell papilloma, lung
1933 23	"	819	109	4,100	Adenocarcinoma, lung
1933 25	"	636	156	5,600	Squamous cell carcinoma, lung
1933 29	"	369	51	1,900	Large lung mass (not examined histologically)
1933 31	"	216	74	1,900	Adenocarcinoma, lung
1933 32	"	501	120	7,500	Squamous cell carcinoma, lung
2086 4	UO ₂ + PuO ₂ ^d	415	97	2,600	Malignant mesothelioma, squamous cell carcinoma, lung
2086 5	"	493	67	2,300	Squamous cell carcinoma, lung
2086 8	"	207	80	1,500	Fibrosarcoma, subcutis
2086 19	"	627	169	8,300	Adenocarcinoma, lung
2086 24	"	284	385	14,000	Radiation pneumonitis, pulmonary fibrosis
2086 25	"	212	321	9,900	Radiation pneumonitis, pulmonary fibrosis
2086 26	"	497	298	16,000	Squamous cell papillomas, lung
2086 28	"	553	101	4,400	Squamous cell carcinoma, lung
2086 29	"	542	138	6,400	Pulmonary fibrosis
2086 31	"	663	157	7,300	Squamous cell carcinoma, lung
2086 32	"	499	144	5,800	Squamous cell carcinoma, lung
2086 34	"	438	7.2	190	Adenocarcinoma, lung
2086 39	"	711	230	9,800	Squamous cell carcinoma, lung
100 15	(U,Pu)O ₂ ^e	427	f	-	Adenocarcinoma, lung
2100 17	"	577	f	-	Squamous cell carcinoma, lung
2100 20	"	557	f	-	Squamous cell carcinoma, lung; malignant mesothelioma
2100 23	"	564	f	-	Lymphocytic leukemia
2100 27	"	607	f	-	Squamous cell carcinoma, lung; malignant mesothelioma
2100 32	"	415	f	-	Adenocarcinoma, lung
2100 36	"	527	f	-	Squamous cell carcinoma, lung
2100 38	"	517	f	-	Squamous cell carcinoma, lung; hemangiosarcoma, lung
2100 39	"	520	f	-	Squamous cell carcinoma, lung
2217 1	PuO ₂ ^g	598	f	-	Squamous cell carcinoma, lung; adenocarcinoma, lung
2217 4	"	528	f	-	Squamous cell papilloma
2217 14	"	700	f	-	Squamous cell carcinoma, lung

Table 3-1 (Continued)

Animal Number	Exposure Aerosol	Survival (DPE) ^b	ILB ^a (nCi)	Cumulative Lung Dose To Death (rads)	Significant Lesions
2217 15	"	511	f	-	Squamous cell carcinoma, lung; adenocarcinoma, lung
2217 18	"	692	f	-	Squamous cell carcinoma, lung; adenocarcinoma, lung
2217 29	"	395	f	-	Hemangiosarcoma, lung
2217 30	"	589	f	-	Hemangiosarcoma, lung
2217 31	"	522	f	-	Hemangiosarcoma, pleura
2217 39	"	597	f	-	Squamous cell carcinoma, lung
2217 49	"	404	f	-	Fibrosarcoma, pleura

^aInitial lung burden of Pu and Am combined, calculated for each animal using sacrifice lung burden and standard retention curve for each radionuclide.

^bDays after exposure.

^cPuO₂ heat-treated at 850°C before mixing with UO₂ and organic binder material, powder obtained from the pellet processing operation at the Babcock and Wilcox plant.

^dPuO₂ calcined at 750°C before mixing with UO₂, powder obtained from the ball milling operation at the Hanford Engineering and Development Laboratory.

^eUO₂ and PuO₂ heat-treated at 1750°C in a reducing atmosphere to produce substoichiometric solid solution, powder obtained from the centerless grinding operation at the Hanford Engineering and Development Laboratory.

^fDetermination of retention functions not completed for determination of initial lung burdens or radiation dose.

^gPuO₂ heat-treated at 850°C, powder obtained from the V-blending process operation at the Babcock and Wilcox plant.

Table 3-2. Dogs Exposed to Mixed (U,Pu) Oxide Aerosols that Died Before Their Scheduled Sacrifice Times

Dog Number	Aerosol Exposure	Survival (DPE) ^a	ILB ^b $\mu\text{Ci/Kg}$	Cumulative Dose to Lung to Death (rads)	Primary Cause of Death	Other Findings
857W	PuO_2^c	1183	1.45	2500	Radiation pneumonitis	Pulmonary fibrosis
901T	PuO_2	1034	1.11	1800	Radiation pneumonitis	Pulmonary fibrosis
803A	$\text{UO}_2 + \text{PuO}_2^d$	1217	1.45	2700	Radiation pneumonitis	Pulmonary adenocarcinoma
823S	$\text{UO}_2 + \text{PuO}_2$	1044	0.36	4800	Pulmonary fibrosis	Pulmonary adenoma
853T	$\text{UO}_2 + \text{PuO}_2$	476	1.10	8600	Radiation pneumonitis	Pulmonary fibrosis
828T	$\text{UO}_2 + \text{PuO}_2$	1825	0.64	2500	Pulmonary fibrosis	Pulmonary adenocarcinoma
888S	$(\text{U,Pu})\text{O}_2^e$	797	0.46	5100	Radiation pneumonitis	Pulmonary fibrosis

^aDays after exposure.

^bInitial lung burden of Pu and Am combined, calculated for each animal using initial lung burden and body weight at exposure.

^c PuO_2 heat-treated at 850°C. Powder was obtained from the pellet processing operation at the Babcock and Wilcox plant.

^d PuO_2 calcined at 750°C before mixing with UO_2 . Powder was obtained from the ball milling operation at the Hanford Engineering and Development Laboratories.

^e UO_2 and PuO_2 heat-treated at 1750°C in a reducing atmosphere to produce substoichiometric solid solution. Powder was obtained from the centerless grinding operation at the Hanford Engineering and Development Laboratories.

Table 3-3. Monkeys Exposed to Mixed (U,Pu) Oxide Aerosols and Sacrificed Longer Than One Year After Exposure

Monkey Number	Aerosol Exposure	Sacrificed DPE ^a	ILB ^b $\mu\text{Ci/Kg}$	Cumulative Dose to Lung to Death (rads)	Lesions
M24	$\text{UO}_2 + \text{PuO}_2^c$	547	0.036	680	No significant lesions
M39	$(\text{U,Pu})\text{O}_2^d$	546	0.098	1750	Alveolar septal fibrosis, mild
M883	PuO_2^e	550	0.058	1190	Alveolar septal fibrosis, mild
M27	$\text{UO}_2 + \text{PuO}_2$	729	0.051	1170	No significant lesions
M38	$(\text{U,Pu})\text{O}_2$	732	0.095	1850	Alveolar septal fibrosis, moderate
M40	PuO_2	730	0.188	4300	Alveolar septal fibrosis, moderate
M25	$\text{UO}_2 + \text{PuO}_2$	1470	0.084	2870	Alveolar septal fibrosis, moderate
M34	$(\text{U,Pu})\text{O}_2$	1486	0.135	4720	Alveolar septal fibrosis, focal
M37	PuO_2	1460	0.099	3410	Alveolar septal fibrosis, severe, widespread

^aDays after exposure.

^bInitial lung burden of Pu and Am combined, calculated for each animal using initial lung burden and body weight at exposure.

^c PuO_2 calcined at 750°C before mixing with UO_2 . Powder was obtained from the ball milling operation at the Hanford Engineering and Development Laboratories.

^d UO_2 and PuO_2 heat-treated at 1750°C in a reducing atmosphere to produce substoichiometric solid solution. Powder was obtained from the centerless grinding operation at the Hanford Engineering and Development Laboratories.

^e PuO_2 heat-treated at 850°C. Powder was obtained from the pellet processing operation at the Babcock and Wilcox plant.

the tumor cells obliterated normal lung architecture, invading vessels, airways, pleura and the thoracic cavity. None of the carcinomas metastasized outside the thoracic cavity. In some cases, the adenocarcinomas were found in the same lungs with squamous cell tumors.

The squamous cell tumors were either benign or malignant. The benign tumors were solitary masses which, on occasion, achieved 2 cm in diameter and compressed adjacent lung parenchyma but did not invade it. Most of the masses were composed of necrotic cells which were sloughed from a thin border of keratinized squamous epithelium at the periphery of the mass. Although these tumors were cystic in nature, they would be classified as squamous cell papillomas using the classification system for rat lung tumors propounded by the International Agency for Research on Cancer (Ref. 3).

The malignant squamous cell tumors were designated squamous cell carcinomas. All were malignant based on cytologic criteria and, in some cases, invasion of adjacent structures. In no case did they metastasize outside the thoracic cavity. About one-third of the squamous cell tumors of all types were multiple or found in the lung with other lung tumor types.

Eight rats had sarcomas of the lung or pleura. Four were hemangiosarcomas primary in the lung and one was a fibrosarcoma of the pleura. Malignant mesotheliomas were found in three cases, always in association with squamous cell carcinoma of the lung. Mesotheliomas are uncommon tumors in the rat and are associated with the implantation or inhalation of fibers or polycyclic hydrocarbons. Inhalation of radioactive materials has only once been reported to cause mesothelioma and that was with inhalation of $^{238}\text{Pu}(\text{NO}_3)_4$ (Ref. 4). This finding leaves the possibility that other nonradioactive carcinogens may be present in the mixed-oxide powders obtained from industrial facilities.

Seven dogs died before their scheduled sacrifice times due to radiation-induced lesions (Table 3-2). The initial lung burdens of Pu expressed in units of $\mu\text{Ci/kg}$ body weight are presented in Table 3-2 as are the cumulative absorbed alpha doses in rads to lung to death.

Considering the initial lung burdens and the times from inhalation exposure to death, the results from these seven dogs are not unique. The initial lung burdens and times to death fall into the ranges observed for dogs exposed to laboratory-produced idealized aerosols of $^{239}\text{PuO}_2$ at this Institute.

The primary cause of death in all seven cases was radiation pneumonitis and pulmonary fibrosis. The radiation pneumonitis was the predominant factor in all but two cases. The inflammatory lesions were similar to others induced by aerosols of laboratory-produced alpha emitters such as PuO_2 . They were characterized by an alveolar accumulation of macrophages and neutrophils, hypertrophy of alveolar lining cells, increased septal thickness due to cellular proliferation and fibrosis, and large parenchymal scars. Most of these lesions were focal but widely spread through the lung.

Although all dogs died of inflammatory lesions, three also had pulmonary tumors (Table 3-2). In the left diaphragmatic lobe of dog 823S, a firm subpleural nodule, 0.5 x 0.4 x 0.3 cm, was found. Thick fibrotic scars were found throughout the lung but were prominent under the pleura. Histologically, the nodule was classified as a pulmonary adenoma. It consisted of hypertrophic alveolar lining cells that were proliferating on a fine stroma. The border of the nodule was a sharp distinction from the normal alveolar structure. Numerous tumor cells were present in the alveolar lumens. The individual cells of the tumor were well differentiated cuboidal and columnar cells that, in some foci, were piled upon one another.

In dog 803A, lung tumors were not noted grossly since pulmonary edema, radiation pneumonitis and pulmonary fibrosis were wide spread and severe. In histologic sections of the right apical and left diaphragmatic lung lobes, widespread radiation pneumonitis and pulmonary fibrosis were

prominent. Around some scars, alveolar lining cells were hypertrophic. In two sections, there were small (about 5 mm diameter) foci where there was dysplasia of the hypertrophic cells. There was a disparity of cell size and maturation and mitoses were frequent. Although they were small foci, the cells filled the alveoli and encroached on surrounding tissues giving the appearance of a pulmonary adenocarcinoma. Metastasis was not found.

Dog 828T was euthanized with severe dyspnea. The lung was small and contracted due to fibrosis. Five small nodules 0.5 to 1 cm in diameter were palpated in the lung. Histologically these were small adenocarcinomas of the lung, bronchioloalveolar pattern, that were associated with pulmonary scars; no metastasis was found.

The lung tumors seen in these dogs were similar to those seen in dogs exposed to $^{238}\text{PuO}_2$ or $^{239}\text{PuO}_2$ (Ref. 5).

No monkeys have died due to radiation related causes in these studies. Animals sacrificed at times greater than 18 months after exposure were examined for histologic lesions. Table 3-3 shows the radiation doses and lesions found in these monkeys. Focal alveolar septal fibrosis was found in most. This ranged in severity and extent from barely perceptible to many small, 1-mm diameter scars. Some alveolar macrophages were associated with the scars but there was no significant inflammatory reaction. In only one instance were alveolar epithelial lining cells hyperplastic. This occurred in one focus over alveolar septa greatly thickened with fibrous tissue.

A comparison of the biologic responses in monkeys and dogs is of interest. Figure 3-1 illustrates the relative lack of response in monkeys compared to dogs. The three monkeys sacrificed at about 1,470 days after exposure had alveolar septal fibrosis that was severe in one case. In contrast, three dogs with survival times and lung doses that bracketed those of the monkeys died with radiation pneumonitis and pulmonary fibrosis. In addition, these three dogs had lung tumors. These findings seem to indicate that monkeys are less sensitive than dogs to inhaled mixed oxides.

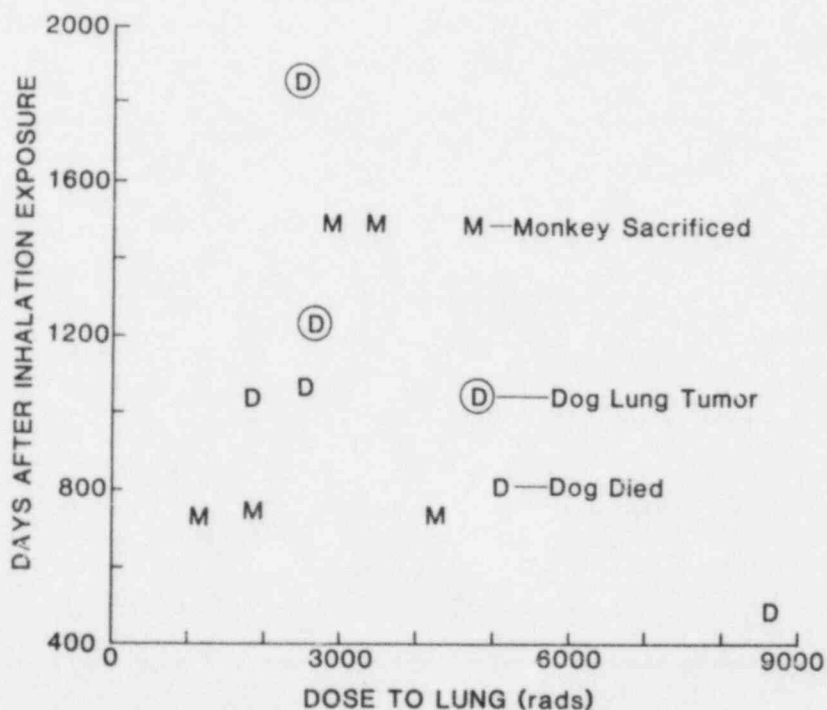


Figure 3-1. Comparison of dogs that died of radiation pneumonitis and pulmonary fibrosis and monkeys sacrificed after inhalation of mixed oxide aerosols. Symbols are M = monkey sacrificed, D = dog died.

REFERENCES

1. Hahn, F. F., J. A. Stanley, A. F. Eidson and J. A. Mewhinney, "Summary of Biological Effects Following Inhalation of Industrial Mixed Oxides (Uranium-Plutonium) or PuO_2 in Rats," in Radiation Dose Estimates and Hazard Evaluations for Inhaled Airborne Radionuclides Annual Report July 1978-July 1979, LMF 71, pp. 67-71, 1980.*
2. Hahn, F. F. and J. A. Mewhinney, "Biologic Effects in Beagle Dogs After Inhalation of Industrial Mixed Oxides (Uranium-Plutonium) or PuO_2 ," in Radiation Dose Estimates and Hazard Evaluations for Inhaled Airborne Radionuclides Annual Report July 1979-June 1980, LMF 86, pp. 42-46, 1981.*
3. Pour, P., M. F. Stanton, M. Kusehner, S. Laskin and L. M. Shabad, "Tumours of the Respiratory Tract," in Pathology of Tumours in Laboratory Animals Volume I - Tumours of the Rat Part 2 V. S. Turusov, ed. International Agency for Research on Cancer, Lyon 1976.
4. Ballou, J. E., G. E. Dagle and K. E. McDonald, "Late Effects of Labeled $\text{Pu}(\text{NO}_3)_4$ in Rats," in Pacific Northwest Laboratory Annual Report for 1976, Part 1. Biomedical Sciences, BNWL 2100, pp. 35-37, 1977.*
5. Mewhinney, J. A., F. F. Hahn, B. B. Boecker, J. H. Diel, R. O. McClellan, J. L. Mauderly, B. B. Muggenburg, J. A. Pickrell and R. A. Guilmette, "Toxicity of Inhaled $^{238}\text{PuO}_2$ in Beagle Dogs," in Inhalation Toxicology Research Institute Annual Report 1980-1981, LMF 91, pp. 150-158, 1981.*

*Available for purchase from the NRC/GPO Sales Program, U. S. Nuclear Regulatory Commission, Washington, DC 20555 or from the National Technical Information Services, Springfield, VA 22161.

4. DOSE RESPONSE STUDIES IN FISCHER-344 RATS

Abstract — Two studies are underway in which groups of Fischer-344 rats have received inhalation exposure to either 1750°C-treated (U,Pu)O₂ or 850°C treated "pure" ²³⁹PuO₂ aerosols to determine the relationship of radiation dose to biological response. In each study, groups of rats were exposed to achieve one of 3 initial lung burdens to produce lung doses of 25, 125, or 625 rads to lung to the median life span. Additional groups of rats are being maintained as controls. This report describes the histopathology observed through 1.75 years after exposure of these groups. Lung retention and tissue distribution of Pu and Am from these aerosols is described for groups of rats sacrificed through 1.5 years after exposure.

PRINCIPAL INVESTIGATORS

J. A. Mewhinney

A. F. Eidson

F. F. Hahn

The objective of this experiment is to determine the relationship of radiation dose to biological response following inhalation of two aerosol forms produced during normal operation of an industrial facility fabricating mixed U-²³⁹Pu nuclear fuel. One aerosol consists of a mixed U-Pu oxide heat-treated to 1750°C; the second aerosol consists of PuO₂ treated at 850°C.

Investigations concerning the fate of inhaled mixed U-Pu oxide; have been under way at this Institute for nearly five years. Three radiation dose pattern studies extending through four years after inhalation have been completed, each using three animal species; Fischer-344 rat, Beagle dog and Cynomolgus monkey (this report pp. 33-40). In these studies, the incidence of lung tumors in Fischer-344 rats has been significant (Ref. 1) and in excess of the incidence reported by Sanders (Ref. 2) following inhalation of ²³⁹PuO₂ by rats at comparable levels of radiation dose.

While significant information exists on the biological effects following inhalation of ²³⁹PuO₂ or UO₂ by rats, dogs and monkeys (Refs. 2,3,4,5) no information exists on the dose-response relationships following inhalation of mixed U-Pu oxides. Specifically, the scientific questions forming the basis for this study are: does the inhalation of aerosols consisting of mixed (U-Pu) oxides pose a unique carcinogenic hazard to lung compared to chemically pure forms of PuO₂ and are the hazard assessments for human inhalation of ²³⁹PuO₂ adequate to be extended to the case of mixed U-Pu oxide inhalation in humans?

METHODS

The experimental design for these studies is summarized in Table 4-1. Methods used in statistical design, inhalation exposure, aerosol characterization and determination of the initial lung for each exposure group have been presented (Ref. 6). Tissue content of Pu was expressed as percentages of the initial lung burden determined from the mean lung content of eight rats from each exposure group sacrificed at seven days after exposure (Ref. 6). Lung retention data were fitted by a nonlinear least squares technique using sums of negative exponential terms. Cumulative percentage survival after exposure was calculated by a life table method (Ref. 7).

RESULTS

The distribution of Pu in tissues of the rat at selected times through 1.5 years after inhalation exposures is presented in Table 4-2 for the (U,Pu)O₂ aerosol material and in Table

Table 4-1. Experimental Design of Dose Response Studies in Fischer-344 Rats that Inhaled (U,Pu)O₂ or "Pure" PuO₂

Lung Dose (rads)	ILB (μCi)		Number of Animals	
	(U,Pu)O ₂	PuO ₂	(U,Pu)O ₂	PuO ₂
625	0.013	0.020	52 ^a	52
125	0.0026	0.005	104(+24 RDP) ^b	104(+24 RDP)
25	0.00052	0.0008	156 ^c	156
Control Rats	0	0	80 ^d	80

^aanimal group = 40(DR*) + 8 (7 day sacrifice) + 4 (spares)
= 1 exposure per aerosol

^banimal group = 80(DR) + 16 (7 day sacrifice) + 8 (spares)
(+ 24 RDP**) = sacrifice animals in RDP study

^canimal group = 120(DR) + 24 (7 day sacrifice) + 12 (spares)
= 3 exposure runs per aerosol

^danimal group = 80 (control)
= 2 exposures per aerosol

*DR = dose response animals.

**RDP = radiation dose pattern animals.

Total number of animals = 832 (3 ILB levels, 2 aerosols, controls).

Total number of exposure runs = 16 (12 for experimental groups, 4 for controls).

Table 4-2. Distribution of Pu in Tissues of Rats Sacrificed at Selected Times After Inhalation Exposure to (U,Pu)O₂.
Data expressed as percentages (mean ± 1 SD) of the initial lung burden.

Tissue	Sacrifice Time (Days After Inhalation)				
	32	64	182	365	548
Lung	34 ± 24	53 ± 91	9.9 ± 9.1	1.1 ± 1.3	2.4 ± 1.7
Liver	3.3 ± 6.7	0.45 ± 0.90	1.9 ± 3.7	ND	0.28 ± 0.55
Kidney	ND ^a	ND	ND	ND	ND
Femur	ND	ND	ND	ND	ND
TBLN	ND	ND	ND	ND	0.39 ± 0.45
Carcass	ND	0.63 ± 1.3	ND	ND	1.6 ± 1.2

^aND = not detectable

4-3 for the "pure" PuO_2 aerosol material. The fitted lung retention functions for Pu for the $(\text{U,Pu})\text{O}_2$ material and for the "pure" PuO_2 material are shown in Figure 4-1. Cumulative percentage survival of rats in these dose-response studies is shown in Figure 4-2. A summary of the status of the rats in each exposure group is shown in Table 4-4. A summary of histopathological findings in rats exposed to these aerosols and dying before April 1, 1982 is presented in Table 4-5.

Table 4-3. Distribution of Pu in Tissues of Rats Sacrificed at Selected Times After Inhalation Exposure to "Pure" PuO_2 .
Data expressed as percentage (mean \pm 1 SD) of the initial lung burden.

Tissue	Sacrifice Time (Days After Inhalation)				
	32	64	182	365	548
Lung	81 \pm 56	27 \pm 15	4.9 \pm 5.6	5.2 \pm 3.8	3.2 \pm 1.4
Liver	0.12 \pm 0.25	0.34 \pm 0.58	ND ^a	0.56 \pm 0.97	0.13 \pm 0.09
Kidney	0.04 \pm 0.08	0.29 \pm 0.14	ND	ND	ND
Femur	0.06 \pm 0.12	ND	ND	ND	ND
TBLN	1.3 \pm 2.2	ND	ND	ND	ND
Carcass	0.10 \pm 0.19	ND	ND	ND	0.15 \pm 0.11

^aND = not detectable

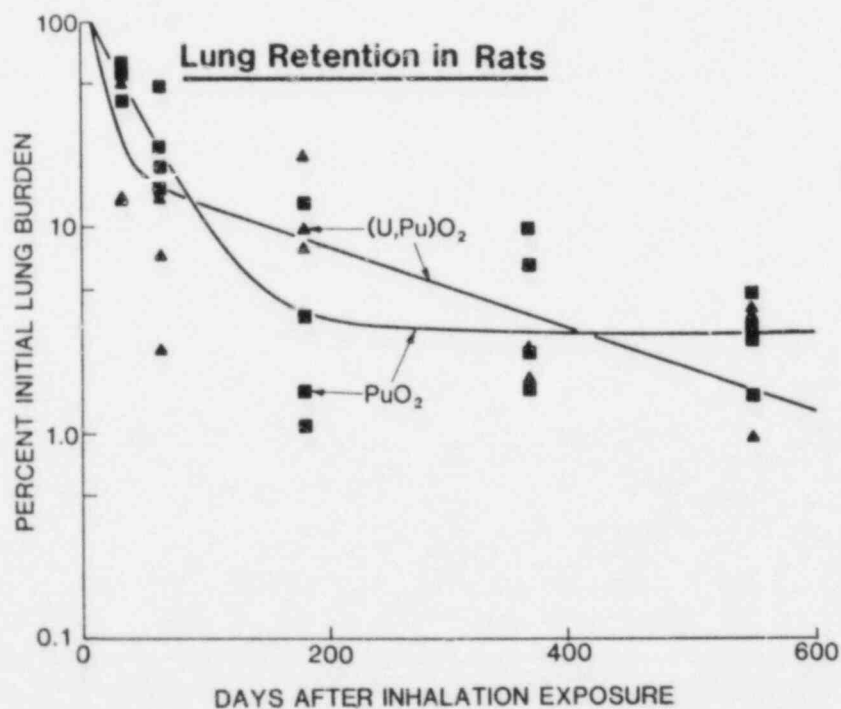


Figure 4-1. Lung retention of $(\text{U,Pu})\text{O}_2$ or "pure" PuO_2 in rats.

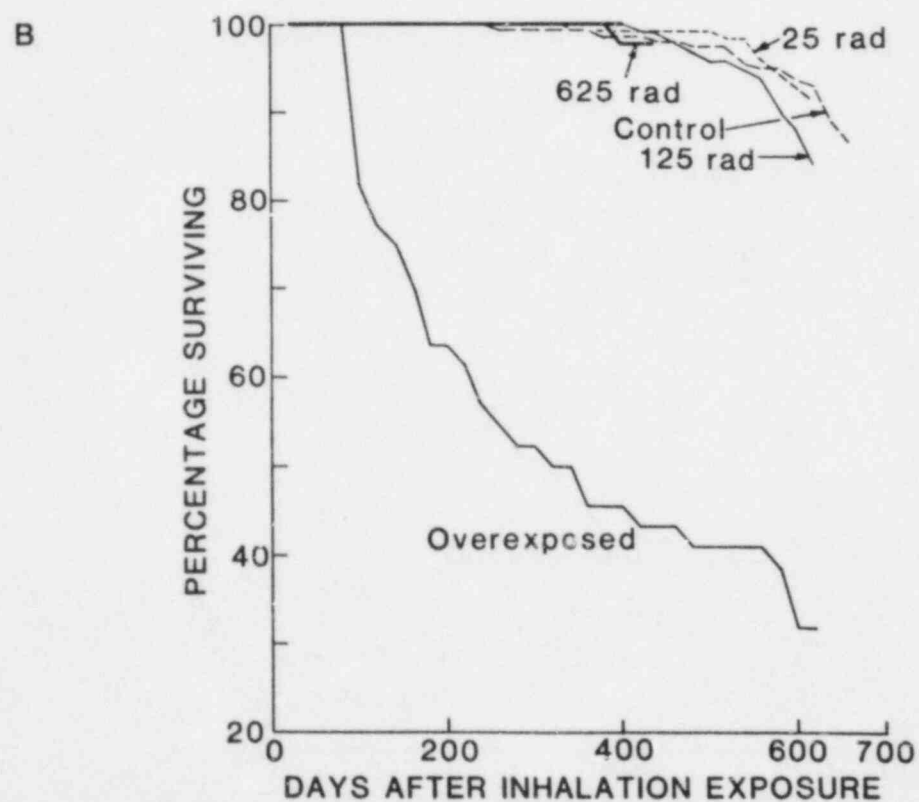
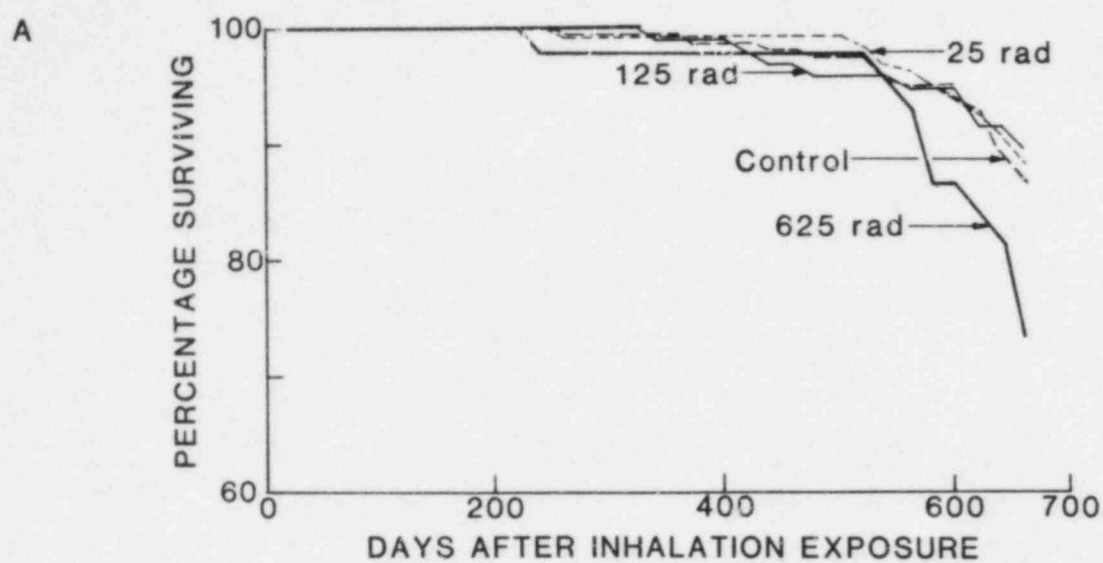


Figure 4-2. Cumulative percentage survival of rats exposed to graded levels of initial lung burden. (a) where inhaled material was $(U,Pu)O_2$ and (b) where inhaled material was "pure" PuO_2 .

Table 4-4. Status of Dose Response Studies in Which Fischer-344 Rats Were
Exposed to Graded ILB Levels of Either (U,Pu)O₂ or "Pure" PuO₂
(On June 30, 1982)

Aerosol	Projected Dose to Lung (rad) ^a	Days After Inhalation	# Animals Entered In Exp.	Number of Deaths	Number Surviving	Percent Survival
(U,Pu)O ₂	25	650	131	14	117	90
	125	651	88	10	78	89
	625	649	44	10	34	77
	Control	649	80	10	70	88
"Pure" Pu	25	611	128	11	117	91
	125	610	88	13	75	85
	625	435	44	1	43	98
	Control	608	80	5	75	94
	Over- exposed	609	44	30	14	32

^aLung dose projected to 900 days after exposure

Table 4-5. Summary of Histopathologic Findings in Rats Exposed to Aerosols of Mixed Oxides and Dying Before April 1, 1982

Experiment	Animal	Death		Pu ILB	Death ^b	
No.	No.	Date	DPE ^a	(nCi)	Type	Comment
2978	031	82033	504	1.38	D	Nephrosis; Testes- interstitial cell tumor
2978	051	82052	523	1.38	D	Lost to followup
2979	094	82086	556	0.302	D	Uremia - nephrosis; Testes - interstitial cell tumor
2980	118	82003	473	1.21	D	Pituitary - adenoma
2980	120	81233	338	1.21	D	Lost to followup
2980	122	81329	434	1.21	D	Mammary gland - adenocarcinoma
2980	140	81312	417	1.21	D	Liver degeneration; Pituitary-adenoma
2981	204	82053	522	0.587	E	Nephrosis; Pituitary - adenoma
2982	267	82076	545	1.29	D	Mononuclear cell leukemia
2983	293	81136	239	19.9	D	No lung sample, cannibalized
2983	326	82083	551	19.9	D	Cannibalized
2983	327	82061	529	19.9	D	Radiation pneumonitis and fibrosis; Lung - adenocarcinoma
2984	010	81157	262	SHAM	D	Nephrosclerosis, severe; Testes - interstitial cell tumor
2984	852	81320	423	SHAM	E	Mammary gland - squamous cell carcinoma
2984	862	82001	469	SHAM	D	No significant lesion
2985	821	81261	364	SHAM	E	No significant lesion
3006	404	82082	511	2.52	D	No lung tumor
3008	498	81275	338	1.21	D	Fibrous, histiocytomas - mediastinum

Table 4-5. Summary of Histopathologic Findings in Rats Exposed to Aerosols of Mixed Oxides and Dying Before April 1, 1982 (Continued)

Experiment	Animal	Death		Pu ILB	Death ^b	
No.	No.	Date	DPE ^a	(nCi)	Type	Comment
3009	003	81036	99	158.5	D	Radiation pneumonitis, pulmonary fibrosis
3009	005	81041	104	158.5	D	Radiation pneumonitis, pulmonary fibrosis
3009	006	81095	158	158.5	D	Radiation pneumonitis and fibrosis
3009	013	81172	235	158.5	D	Radiation pneumonitis and fibrosis, Adrenal - pleochromocytoma
3009	021	81092	155	158.5	D	Radiation pneumonitis and fibrosis
3009	022	81034	97	158.5	D	Radiation pneumonitis and fibrosis
3009	024	81109	172	158.5	D	Radiation pneumonitis and fibrosis
3009	027	81035	98	158.5	D	Radiation pneumonitis and fibrosis
3009	028	81069	132	158.5	D	Radiation pneumonitis and fibrosis
3009	031	81103	166	158.5	D	Radiation pneumonitis and fibrosis
3009	032	81107	170	158.5	D	Lost to followup
3009	043	81138	201	158.5	D	Radiation pneumonitis and fibrosis
3009	044	81047	110	158.5	D	Lost to followup
3009	046	81033	96	158.5	D	Radiation pneumonitis and fibrosis

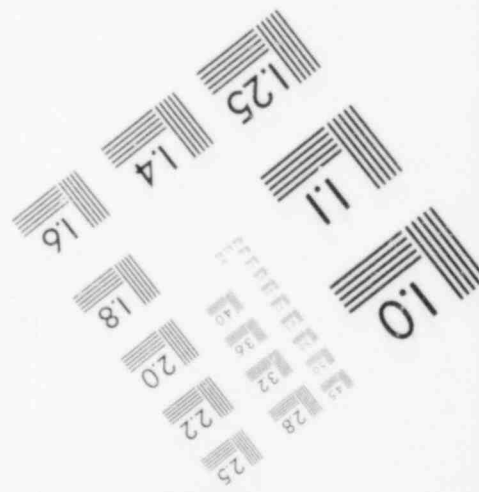
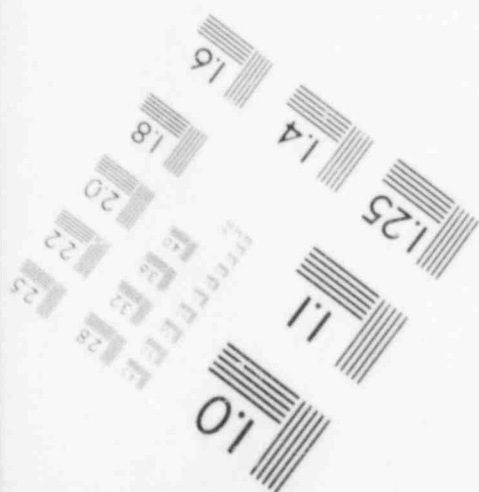
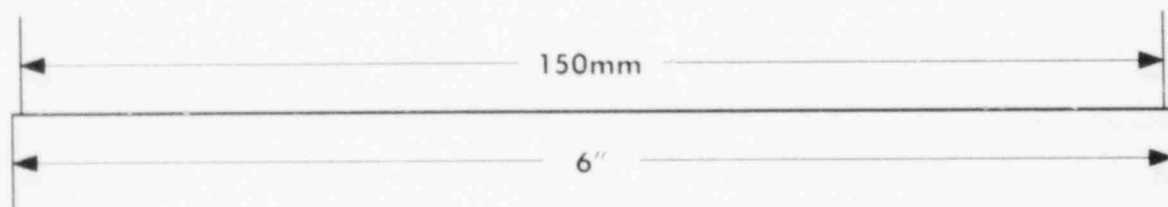
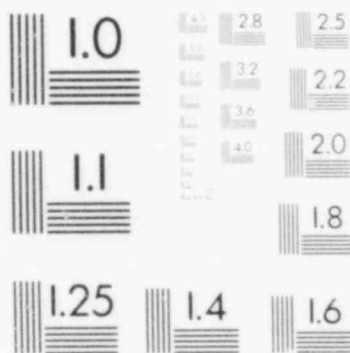
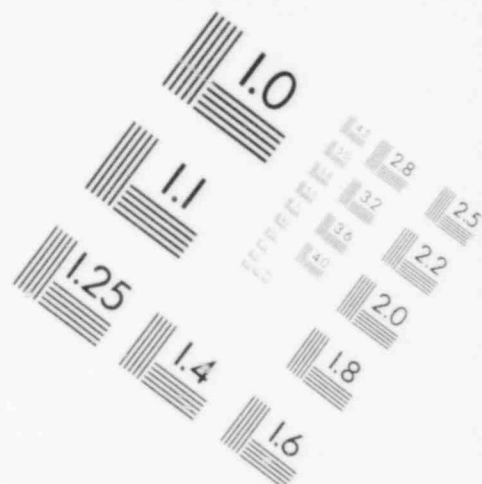
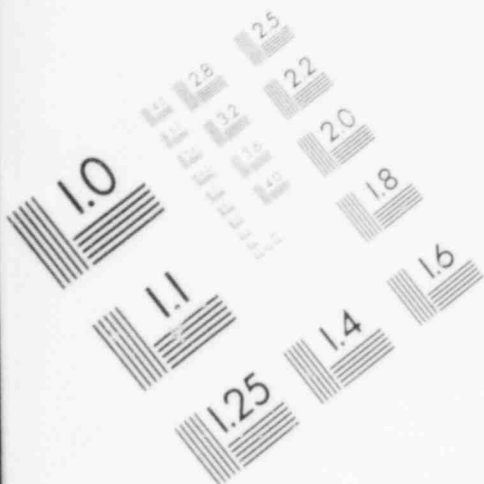
Table 4-5. Summary of Histopathologic Findings in Rats Exposed to Aerosols of Mixed Oxides and Dying Before April 1, 1982 (Continued)

Experiment	Animal	Death		Pu ILB	Death ^b	
No.	No.	Date	DPE ^a	(nCi)	Type	Comment
3009	047	81172	235	158.5	D	Radiation pneumonitis and fibrosis
3009	048	81028	91	158.5	D	Radiation pneumonitis and fibrosis; nephrosis
3009	051	81031	94	158.5	D	Radiation pneumonitis and fibrosis
3009	052	81030	93	158.5	D	Radiation pneumonitis and fibrosis
3009	531	81297	360	158.5	D	Radiation pneumonitis and fibrosis; Lung - squamous cell carcinoma
3009	537	81197	260	158.5	D	Radiation pneumonitis and fibrosis
3009	535	81245	308	158.5	D	Radiation pneumonitis and fibrosis
3009	539	81201	264	158.5	D	Radiation pneumonitis and fibrosis
3009	546	81338	401	158.5	E	Pulmonary fibrosis
3009	556	81297	360	158.5	D	Radiation pneumonitis and fibrosis; Lung - squamous cell carcinoma
3010	688	81352	413	10.0	D	Lost to followup
3011	722	82020	446	6.94	D	Radiation pneumonitis
3011	735	82060	486	6.94	D	Adrenal - ganglioneuroma
3011	761	82042	468	6.94	D	Lung - adenocarcinoma

^aDPE = Days Past Exposure

^bD = Died E = Euthanized

IMAGE EVALUATION
TEST TARGET (MT-3)



DISCUSSION

The distribution of Pu in tissues of animals sacrificed at times through 1.5 years after exposure clearly indicate the insoluble nature of these two aerosols. Only very small quantities of Pu have solubilized in lung and transport to liver or skeleton. Preliminary fitting of the lung retention data for Pu using two component sums of negative exponentials did not indicate a significant difference between the two aerosols. There is an indication that mechanical clearance from the respiratory tract, as estimated by comparing the lung retention half time estimated by the first component of the retention equation, may occur more rapidly in these rats than for comparable groups in the radiation dose pattern studies (this report pp. 33-40). This could be due to the somewhat larger particle size measured during inhalation exposure in these studies, leading to more rapid clearance rates. More definitive comparisons using the biomathematical model (this report pp. 21-32) will be made when radiochemical analysis of excreta samples are complete.

Survival percentages for all experimental groups are not different from the control (sham exposed) groups through 1.5 years after inhalation exposure (Table 4-4 and Fig. 4-2) with the exception noted below. The survival data indicate that the experimental design criteria are being met, since at the levels of dose-to-lung used in these studies, no early mortality due to radiation pneumonitis and pulmonary fibrosis was expected. In the single group of animals which inadvertently received an inhalation exposure to "pure" PuO_2 much greater than planned, significant early mortality has been observed. This over-exposed group has since been replaced by a properly exposed group. The primary cause of death in the over-exposed group (projected lung dose of 5000 rads at 900 days after inhalation) has been radiation pneumonitis and pulmonary fibrosis.

Histopathological evaluations are complete on all animals dying or sacrificed before April 1, 1982. In the sacrificed animals, no lesions attributable to absorbed radiation dose were observed.

Twenty-seven rats died or were euthanized in the dose response studies. Three sham exposed, control rats died, one with a squamous cell carcinoma of the mammary gland and two with no significant gross or microscopic lesions in the major organ systems. At 364-469 days after exposure to either $(\text{U, Pu})\text{O}_2$ or "pure" PuO_2 , three animals were lost to followup because of autolysis or cannibalism.

Seven rats from the over-exposed group with a mean lung burden of 158 nCi of Pu died due to radiation pneumonitis and pulmonary fibrosis, as did one rat with 19.9 nCi ILB. They died from 260 to 529 days after exposure. Four of these eight rats also had lung tumors, two squamous cell carcinomas, one adenosquamous carcinoma and one squamous cell adenoma. One other lung tumor was found, an adenocarcinoma, in a rat with 6.94 nCi ILB. The four carcinomas were malignant by histologic criteria, but there were no distant metastases. The squamous cell adenoma was a large tumor that was space-occupying but was histologically benign with a large keratinized cystic center.

The other lesions found could not be directly related to radiation injury. Pituitary adenomas, testicular interstitial cell tumors, mononuclear cell leukemia, nephrosis, liver degeneration and biliary hyperplasia are all common aging lesions in Fischer-344 rats (Refs. 8,9).

Three tumors noted are unusual but cannot be directly related to radiation injury. Fibrous histiocyctomas have been reported in Fischer-344 rats but never from the mediastinum (Ref. 10). Ganglioneuromas of the adrenals are rare tumors (Ref. 11) as are oligodendrogliomas (Ref. 12).

These preliminary results and analyses indicated that these studies are progressing according to the initial experimental design. Mortality has been low in the experimental groups as expected. Critical information to assess the potential risk due to inhalation of $(\text{U,Pu})\text{O}_2$ and "pure" PuO_2 compared to pure forms of actinide elements should become available during the next year.

REFERENCES

1. Hahn, F. F., J. A. Stanley, A. F. Eidson and J. A. Mewhinney, "Summary of Biological Effects Following Inhalation of Industrial Mixed Oxides (Uranium-Plutonium) or PuO_2 in Rats," in Radiation Dose Estimates and Hazard Evaluations for Inhaled Airborne Radionuclides, Annual Progress Report, July 1, 1978-June 30, 1979, NUREG/CR-1458, LF-71, 61-71, 1980.
2. Sanders, C. L., C. E. Dagle, W. C. Cannon, D. K. Craig, G. J. Powers and D. M. Meier, "Inhalation Carcinogenesis of High-Fired $^{239}\text{PuO}_2$ in Rats," Radiat. Res. 68: 349-360, 1976.
3. Sanders, C. L., C. E. Dagle, W. C. Cannon, G. J. Powers and D. M. Meier, "Inhalation Carcinogenesis of High Fired $^{238}\text{PuO}_2$ in Rats," Radiat. Res. 71: 528-546, 1977.
4. Bair, W. J. and R. C. Thompson, "Plutonium: Biomedical Research," Science 183: 715-722, 1974.
5. Leach, L. J., C. L. Yuile, H. C. Hodge, G. E. Sylvester and H. B. Wilson, "A Five-Year Inhalation Study with Natural Uranium Dioxide (UO_2) Dust. II. Postexposure Retention and Biologic Effects in the Monkey, Dog and Rat," Health Phys. 25: 239-258, 1973.
6. Mewhinney, J. A., A. F. Eidson, F. F. Hahn and W. C. Griffith, "Dose Response Studies in Fischer-344 Rats," in Radiation Dose Estimates and Hazard Evaluation for Inhaled Airborne Radionuclides, Annual Progress Report, July 1, 1980-June 30, 1981, NUREG/CR-2512, LMF-92, 1982.
7. Cutler, S. J. and F. Ederer, "Maximum Utilization of the Life Table Method in Analyzing Survival," J. Chronic. Dis. 8: 699-712, 1958.
8. Goodman, D. G., J. M. Ward, R. A. Squire, K. C. Chu and M. S. Linhart, "Neoplastic and Non-Neoplastic Lesions in Aging Fischer-344 Rats," Toxicol. Appl. Pharmacol. 48: 237-248, 1979.
9. Coleman, G. L., S. W. Barthold, G. W. Osbaldiston, S. J. Foster and A. M. Jonas, "Pathological Changes During Aging in Barrier-Reared Fischer-344 Male Rats," J. Gerontol. 32: 258-278, 1977.
10. Ward, J. M., B. A. Kulwich, G. Reznik and J. J. Berman, "Malignant Fibrous Histiocytoma," Arch. Path. Lab. Med. 105: 313-316 (1981).
11. Fitzgerald, J. E., J. L. Schardein and S. M. Kurtz, "Spontaneous Tumors of the Nervous System in Albino Rats," J. Natl. Cancer Inst. 52: 265-273 (1974).
12. Bots, G., Tb, A. M., R. Kroes and V. J. Feron, "Spontaneous Tumors of the Brain of Rats," Pathol. Vet. 5: 290-296 (1968).

APPENDIX A

Status of Inhalation Studies

	<u>Page</u>
Status of Inhalation Studies of Aerosols of PuO_2 Heat-treated at 750°C Mixed with UO_2 and Ball Milled at HEDL in Beagle Dogs, Monkeys and Fischer-344 Rats.....	52
Status of Inhalation Studies of 1750°C Heat-treated $(\text{U,Pu})\text{O}_{1.96}$ Aerosols from the Pellet Grinding Operation at HEDL in the Beagle Dogs, Monkeys and Fischer-344 Rats.....	54
Status of Inhalation Studies of 850°C Heat-treated PuO_2 Aerosols from the V-Blending Operation at Babcock and Wilcox in Beagle Dogs, Monkeys and Fischer-344 Rats.....	56
Status of Inhalation Studies of 850°C Heat-treated PuO_2 , Mixed with UO_2 and Organic Binders (pellet pressing at Babcock and Wilcox) in Fischer-344 Rats (Pilot Study).....	58

STATUS OF INHALATION STUDIES OF AEROSOLS OF PU02 HEAT-TREATED AT 750 C. MIXED
WITH UO2 AND BALL MILLED AT HEDL IN BEAGLE DOGS, MONKEYS AND FISCHER-344 RATS

SPECIES	NUMBER				EXPOSURE		EXP.		AEROSOL SIGMA	PROJ. DEATH SAC. DATE	DPE	ALIVE DPE 6-30-82	COMMENT
	TT00	RADT0.	SEX	DATE	AGE (DAYS)	WT. (KG)	AMAD (UM)						
BEAGLE DOG	871C	1935-01	M	76344	708	9.90	2.19	1.91		0	76344	0	S-
BEAGLE DOG	219C	1935-02	M	76344	3629	10.1	2.15	1.74		4	76348	4	S-
BEAGLE DOG	635B	1935-03	M	76344	1656	11.4	1.84	1.68		4	76348	4	S-
BEAGLE DOG	821T	1936-02	F	76345	884	8.5	1.68	1.65		549	78165	551	S-
BEAGLE DOG	217E	1937-01	M	76349	3648	8.1	2.41	1.70		0	76349	0	S-
BEAGLE DOG	817T	1937-02	F	76349	892	8.2	2.04	1.74		64	77047	64	S-
BEAGLE DOG	823S	1937-03	F	76349	886	7.2	2.50	1.77			79297	1044	E-LTR
BEAGLE DOG	812A	1937-04	M	76349	896	9.3	2.33	1.73		1462	80350	1462	S-
BEAGLE DOG	803A	1938-01	M	76350	910	10.5	2.10	1.67			80106	1217	D-LTR
BEAGLE DOG	810U	1938-02	F	76350	901	8.0	2.61	2.38		1462	80351	1462	S-
BEAGLE DOG	811B	1938-03	M	76350	897	10.2	2.67	1.62					2023 LTR
BEAGLE DOG	804A	1938-04	M	76350	910	10.9	2.47	1.58		64	77049	65	S-
BEAGLE DOG	828T	1939-01	F	76351	872	6.9	2.18	1.66			81349	1825	E-LTR
BEAGLE DOG	811A	1939-02	M	76351	898	12.8	2.18	1.71		730	78349	729	S-
BEAGLE DOG	799B	1939-03	M	76351	929	11.7	2.34	1.73		365	77350	365	S-
BEAGLE DOG	825S	1940-01	F	76352	889	9.3	2.22	1.73		730	78352	731	S-
BEAGLE DOG	826T	1940-02	F	76352	884	11.0	1.79	1.81		365	77353	367	S-
BEAGLE DOG	802D	1940-03	M	76352	915	8.3	2.35	1.96		549	78170	549	S-
RHESUS MONKEY	917	2087-01	M	77039	5-7YRS-B	4.85	1.61	1.62		0	77039	0	S-
CYNOMOLGUS MONKEY	25	2087-02	M	77039	3-5YRS	3.15	1.53	1.53		1462	81048	1470	S-
CYNOMOLGUS MONKEY	21	2088-01	M	77040	5-7YRS	4.4	1.10	1.34		64	77104	64	S-
CYNOMOLGUS MONKEY	26	2088-02	M	77040	3-5YRS-B	3.7	1.37	1.56		365	78040	365	S-
CYNOMOLGUS MONKEY	24	2088-03	M	77040	3-5YRS-B	3.6	1.22	1.55		549	78222	547	S-
RHESUS MONKEY	918	2089-01	M	77041	5-7YRS-B	4.4	1.61	1.53		4	77045	4	S-
CYNOMOLGUS MONKEY	27	2089-02	M	77041	3-5YRS-B	3.4	1.41	1.56		730	79040	729	S-
CYNOMOLGUS MONKEY	22	2089-03	F	77041	3-4YRS-B	2.5	1.25	1.59			78056	380	D-GASTRIC TORSION
RHESUS MONKEY	897	2090-01	M	77046	5-7YRS-B	4.6	2.13	2.30			78211	530	D-FIB.PLEURITIS
FISCHER-344 RATS	2086-01	M	77042	9WKS			2.32	1.77		0	77042	0	S-
FISCHER-344 RATS	2086-02	M	77042	9WKS			2.32	1.77		365	78044	367	S-
FISCHER-344 RATS	2086-03	M	77042	9WKS			2.32	1.77			79017	705	D-
FISCHER-344 RATS	2086-04	M	77042	9WKS			2.32	1.77			78094	417	D-MAL.MESO THORAX
FISCHER-344 RATS	2086-05	M	77042	9WKS			2.32	1.77			78170	493	D-SQU.CELL CARC.
FISCHER-344 RATS	2086-06	M	77042	9WKS			2.32	1.77		4	77046	4	S-
FISCHER-344 RATS	2086-07	M	77042	9WKS			2.32	1.77		365	79044	367	S-
FISCHER-344 RATS	2086-08	M	77042	9WKS			2.32	1.77			77249	207	E-FIB.SUB.
FISCHER-344 RATS	2086-09	M	77042	9WKS			2.32	1.77		730	79043	731	S-
FISCHER-344 RATS	2086-10	M	77042	9WKS			2.32	1.77		4	77046	4	S-UNEXP.CONTROL
FISCHER-344 RATS	2086-11	M	77042	9WKS			2.32	1.77		365	78044	367	S-
FISCHER-344 RATS	2086-12	M	77042	9WKS			2.32	1.77		0	77042	0	S-
FISCHER-344 RATS	2086-13	M	77042	9WKS			2.32	1.77		0	77042	0	S-
FISCHER-344 RATS	2086-14	M	77042	9WKS			2.32	1.77		64	77105	63	S-
FISCHER-344 RATS	2086-15	M	77042	9WKS			2.32	1.77		4	77046	4	S-

B-PRIMATE CAUGHT IN THE WILD; AGE ESTIMATED FROM BODY WEIGHT AT EXPOSURE

D-SPONTANEOUS DEATH

E-EUTHANIZED

S-SACRIFICED

LTR-LONG TERM RESERVE

STATUS OF INHALATION STUDIES OF AEROSOLS OF PU02 HEAT-TREATED AT 750 C. MIXED WITH
U02 AND BALL MILLED AT HEDL IN BEAGLE DOGS, MONKEYS AND FISCHER-344 RATS (CONTINUED)

SPECIES	NUMBER		SEX	DATE	EXPOSURE		EXP. AMAD (UM)	AEROSOL SIGMA	PROJ. DEATH		DPE	ALIVE DPE		COMMENT
	TYOC	RADIO.			AGE (DAYS)	WT. (KG)			SAC. DATE	DPE		6-30-82		
FISCHER-344 RATS		2086-16	M	77042	9WKS		2.32	1.77	4	77046	4			S-
FISCHER-344 RATS		2086-17	M	77042	9WKS		2.32	1.77	4	77046	4			S-
FISCHER-344 RATS		2086-18	M	77042	9WKS		2.32	1.77	64	77105	63			S-
FISCHER-344 RATS		2086-19	M	77042	9WKS		2.32	1.77		78304	627			D-ADENO.LUNG
FISCHER-344 RATS		2086-20	M	77042	9WKS		2.32	1.77	64	77105	63			S-
FISCHER-344 RATS		2086-21	F	77042	9WKS		2.32	1.77	547	78223	546			S-
FISCHER-344 RATS		2086-22	F	77042	9WKS		2.32	1.77	730	79043	731			S-
FISCHER-344 RATS		2086-23	F	77042	9WKS		2.32	1.77	0	77042	0			S-
FISCHER-344 RATS		2086-24	F	77042	9WKS		2.32	1.77		77326	284			D-RAD.PNEUM.,PUL.FIB.
FISCHER-344 RATS		2086-25	F	77042	9WKS		2.32	1.77		77254	212			D-RAD.PNEUM.,PUL.FIB.
FISCHER-344 RATS		2086-26	F	77042	9WKS		2.32	1.77		78174	497			D-SQU.CELL PAPILLOMA
FISCHER-344 RATS		2086-27	F	77042	9WKS		2.32	1.77	365	78044	367			S-
FISCHER-344 RATS		2086-28	F	77042	9WKS		2.32	1.77		78230	553			D-SQU.CELL CARC.
FISCHER-344 RATS		2086-29	F	77042	9WKS		2.32	1.77		78219	542			D-PUL.FIBROSIS
FISCHER-344 RATS		2086-30	F	77042	9WKS		2.32	1.77	730	79043	731			S-
FISCHER-344 RATS		2086-31	F	77042	9WKS		2.32	1.77		78340	663			D-SQU.CELL CARC.
FISCHER-344 RATS		2086-32	F	77042	9WKS		2.32	1.77		78176	499			D-SQU.CELL CARC.
FISCHER-344 RATS		2086-33	F	77042	9WKS		2.32	1.77	547	78223	546			S-
FISCHER-344 RATS		2086-34	F	77042	9WKS		2.32	1.77		78115	438			D-ADENO.LUNG
FISCHER-344 RATS		2086-35	F	77042	9WKS		2.32	1.77	0	77042	0			S-
FISCHER-344 RATS		2086-36	F	77042	9WKS		2.32	1.77	365	78044	367			S-
FISCHER-344 RATS		2086-37	F	77042	9WKS		2.32	1.77	64	77105	63			S-
FISCHER-344 RATS		2086-37	F	77042	9WKS		2.32	1.77	64	77105	63			S-
FISCHER-344 RATS		2086-38	F	77042	9WKS		2.32	1.77		79023	711			D-SQU.CELL CARC.
FISCHER-344 RATS		2086-40	F	77042	9WKS		2.32	1.77	730	79043	731			S-

B-PRIMATE CAUGHT IN THE WILD, AGE ESTIMATED FROM BODY WEIGHT AT EXPOSURE
D-SPONTANEOUS DEATH
E-EUTHANIZED
S-SACRIFICED
LTR-LONG TERM RESERVE

STATUS OF INHALATION STUDIES OF 1750 C HEAT-TREATED (U,P)01.96 AEROSOLS FROM THE
 PELLET GRINDING OPERATION AT HEDL IN BEAGLE DOGS, MONKEYS AND FISCHER-344 RATS

SPECIES	NUMBER		SEX	DATE	EXPOSURE		EXP. AMAD	AEROSOL SIGMA	PROJ. DEATH		DPE	ALIVE DPE		COMMENT
	TT00	RADIO.			(DAYS)	WT. (KG)			SAC.	DATE		6-30-82		
BEAGLE DOG	634A	2118-01	M	77083	1761	13.0	2.6	2.4	0	77083	0			S-
BEAGLE DOG	643A	2118-02	M	77083	1725	9.8	2.4	1.7	4	77087	4			S-
BEAGLE DOG	7770	2118-03	M	77083	1167	9.5	2.5	1.6	64	77147	64			S-
BEAGLE DOG	640S	2119-01	F	77084	1745	10.3	2.2	1.6	0	77084	0			S-
BEAGLE DOG	641S	2119-02	F	77084	1730	11.4	1.3	1.7	4	77088	4			S-
BEAGLE DOG	796S	2119-03	F	77084	1037	10.0	2.6	1.6	64	77147	63			S-
BEAGLE DOG	783B	2120-01	M	77088	1102	8.7	2.4	1.6	365	78088	365			S-
BEAGLE DOG	789A	2120-02	M	77088	1069	10.3	2.3	1.7	547	78270	547			S-
BEAGLE DOG	883C	2120-03	M	77088	763	9.8	2.4	1.7		82167	1905			E-LTR
BEAGLE DOG	961B	2122-01	M	77090	524	12.0	3.1	1.8	730	79089	729			S-
BEAGLE DOG	797S	2122-02	F	77090	1035	8.3	2.7	1.6	365	78090	365			S-
BEAGLE DOG	798T	2122-03	F	77090	1034	8.6	2.6	1.6	547	78272	547			S-
BEAGLE DOG	791A	2123-01	M	77091	1063	9.3	2.4	1.7	1462	81092	1462			S-
BEAGLE DOG	802U	2123-02	F	77091	1020	9.2	2.9	1.8	730	79092	731			S-
BEAGLE DOG	853T	2124-01	F	77096	900	9.6	2.9	1.9		78207	476			D-LTR
BEAGLE DOG	863C	2124-02	M	77096	857	10.2	2.8	1.7				1911		LTR
BEAGLE DOG	803S	2124-03	F	77096	1022	9.4	2.6	1.8	1462	81100	1465			S-
BEAGLE DOG	888S	2124-04	F	77096	754	8.2	2.9	1.7		79163	797			D-LTR
CYNOMOLGUS MONKEY	36	2256-01	M	77236	3-5YRS-B	3.3	2.0	1.6	365	78236	365			S-
RHESUS MONKEY	900	2257-01	M	77237	5-7YRS-B	7.5	2.3	1.7	0	77237	0			S-
CYNOMOLGUS MONKEY	35	2257-02	M	77237	3-5YRS-B	3.7	2.5	1.7	64	77301	64			S-
CYNOMOLGUS MONKEY	39	2257-03	M	77237	3-5YRS-B	3.1	2.4	1.7	547	79053	546			S-
CYNOMOLGUS MONKEY	38	2257-04	M	77237	3-5YRS-B	3.2	2.4	1.7	730	79239	732			S-
RHESUS MONKEY	914	2258-01	M	77238	5-7YRS-B	7.0	2.3	1.8	4	77242	4			S-
CYNOMOLGUS MONKEY	34	2258-02	M	77238	3-5YRS-B	3.8	2.5	1.7	1462	81245	1468			S-
CYNOMOLGUS MONKEY	31	2258-03	M	77238	3-5YRS-B	3.8	2.4	1.7				1769		LTR
CYNOMOLGUS MONKEY	44	2258-04	M	77238	5-7YRS-B	4.7	2.8	1.7				1769		LTR
FISCHER-344 RAT		2100-01	F	77055	9WKS		2.3	1.7	547	78237	547			S-
FISCHER-344 RAT		2100-02	F	77055	9WKS		2.3	1.7	0	77055	0			S-
FISCHER-344 RAT		2100-03	F	77055	9WKS		2.3	1.7	730	79058	733			S-
FISCHER-344 RAT		2100-04	F	77055	9WKS		2.3	1.7	64	77119	64			S-
FISCHER-344 RAT		2100-05	F	77055	9WKS		2.3	1.7	365	78055	365			S-
FISCHER-344 RAT		2100-06	M	77055	9WKS		2.3	1.7	64	77119	64			S-
FISCHER-344 RAT		2100-07	F	77055	9WKS		2.3	1.7	365	78055	365			S-
FISCHER-344 RAT		2100-08	F	77055	9WKS		2.3	1.7	64	77119	64			S-
FISCHER-344 RAT		2100-09	F	77055	9WKS		2.3	1.7	0	77055	0			S-
FISCHER-344 RAT		2100-10	M	77055	9WKS		2.3	1.7	4	77059	4			S-
FISCHER-344 RAT		2100-11	F	77055	9WKS		2.3	1.7	547	78237	547			S-
FISCHER-344 RAT		2100-12	F	77055	9WKS		2.3	1.7	730	79058	733			S-
FISCHER-344 RAT		2100-13	F	77055	9WKS		2.3	1.7		78198	508			D-
FISCHER-344 RAT		2100-14	F	77055	9WKS		2.3	1.7	365	78055	365			S-
FISCHER-344 RAT		2100-15	F	77055	9WKS		2.3	1.7		78117	427			D-ADENO.LUNG
FISCHER-344 RAT		2100-16	F	77055	9WKS		2.3	1.7	4	78059	4			S-
FISCHER-344 RAT		2100-17	F	77055	9WKS		2.3	1.7		78267	577			D-SQU.CELL CARC.LUNG

B-PRIMATE CAUGHT IN THE WILD; AGE ESTIMATED FROM BODY WEIGHT AT EXPOSURE

D-SPONTANEOUS DEATH

E-EUTHANIZED

S-SACRIFICED

LTR-LONG TERM RESERVE

STATUS OF INHALATION STUDIES OF 1750 C HEAT-TREATED (U₂PU)01.96 AEROSOLS FROM THE PELLET
GRINDING OPERATION AT HEDL IN BEAGLE DOGS, MONKEYS AND FISCHER-344 RATS (CONTINUED)

SPECIES	NUMBER		SEX	DATE	EXPOSURE	WT. (KG)	EXP. AMAD (UM)	AEROSOL SIGMA	PROJ. DEATH SAC. DATE	DPE	ALIVE DPE 6-30-82	COMMENT
	TT00	RADIO.			AGE (DAYS)							
FISCHER-344 RAT	2100-18	F	77055	9WKS			2.3	1.7	0	77055	0	S-
FISCHER-344 RAT	2100-19	F	77055	9WKS			2.3	1.7	730	79058	733	S-
FISCHER-344 RAT	2100-20	F	77055	9WKS			2.3	1.7		78247	557	D-SQU.CELL CARC.LUNG
FISCHER-344 RAT	2100-21	M	77055	9WKS			2.3	1.7	64	77119	64	S-
FISCHER-344 RAT	2100-22	M	77055	9WKS			2.3	1.7	365	78055	365	S-
FISCHER-344 RAT	2100-23	M	77055	9WKS			2.3	1.7		78254	564	D-LYMPH.LEUKEMIA
FISCHER-344 RAT	2100-24	M	77055	9WKS			2.3	1.7	0	77055	0	S-
FISCHER-344 RAT	2100-25	M	77055	9WKS			2.3	1.7	0	77055	0	S-
FISCHER-344 RAT	2100-26	M	77055	9WKS			2.3	1.7	0	77055	0	S-
FISCHER-344 RAT	2100-27	M	77055	9WKS			2.3	1.7		78297	607	D-SQU.CELL CARC.LUNG
FISCHER-344 RAT	2100-28	M	77055	9WKS			2.3	1.7		77055	0	D-DURING EXPOSURE
FISCHER-344 RAT	2100-29	M	77055	9WKS			2.3	1.7		77055	0	D-DURING EXPOSURE
FISCHER-344 RAT	2100-30	F	77055	9WKS			2.3	1.7	4	77059	4	S-
FISCHER-344 RAT	2100-31	M	77055	9WKS			2.3	1.7	730	79058	733	S-
FISCHER-344 RAT	2100-32	M	77055	9WKS			2.3	1.7		78105	415	D-ADENO.LUNG
FISCHER-344 RAT	2100-33	M	77055	9WKS			2.3	1.7	547	78237	547	S-
FISCHER-344 RAT	2100-34	M	77055	9WKS			2.3	1.7	64	77119	64	S-
FISCHER-344 RAT	2100-35	M	77055	9WKS			2.3	1.7	4	77059	4	S-
FISCHER-344 RAT	2100-36	M	77055	9WKS			2.3	1.7		78217	527	D-SQU.CELL CARC.LUNG
FISCHER-344 RAT	2100-37	M	77055	9WKS			2.3	1.7	4	77059	4	S-
FISCHER-344 RAT	2100-38	M	77055	9WKS			2.3	1.7		78207	517	D-SQU.CELL CARC.LUNG
FISCHER-344 RAT	2100-39	M	77055	9WKS			2.3	1.7		78210	520	D-SQU.CELL CARC.LUNG
FISCHER-344 RAT	2100-40	M	77055	9WKS			2.3	1.7	547	78237	547	S-

B-PRIMATE CAUGHT IN THE WILD, AGE ESTIMATED FROM BODY WEIGHT AT EXPOSURE

D-SPONTANEOUS DEATH

E-EUTHANIZED

S-SACRIFICED

LTR-LONG TERM RESERVE

STATUS OF INHALATION STUDIES OF H50 C HEAT-TREATED PU02 AEROSOLS FROM THE V-BLENDING
OPERATION AT BARCOCK AND WILCOX IN BEAGLE DOGS, MONKEYS AND FISCHER-344 RATS

SPECIES	NUMBER	TT00	RADIO	SEX	DATE	EXPOSURE		EXP. AEROSOL	SIGMA	PROJ. DEATH		DPE	ALIVE DPE	COMMENT
						AGE (DAYS)	WT. (KG)			SAC. DATE	DATE			
BEAGLE DOG	7910	2218-01	M	77193	1166	8.2	2.4	1.9	365	78193	365	6-30-82		S-
BEAGLE DOG	902A	2218-02	M	77193	806	8.9	2.3	1.9					1814	LTR
BEAGLE DOG	974U	2218-03	F	77193	602	7.9	2.4	1.8	64	77257	64			S-
BEAGLE DOG	839S	2219-01	F	77194	1058	8.6	2.1	1.7		77196	2			D-LTR
BEAGLE DOG	837S	2220-01	F	77195	1059	9.7	2.0	1.7	0	77195	0			S-
BEAGLE DOG	843I	2220-02	F	77195	1055	9.7	2.2	1.8	730	79194	729			S-
BEAGLE DOG	789C	2220-03	M	77195	1176	12.2	2.0	1.8	64	77259	64			S-
BEAGLE DOG	838S	2221-01	F	77196	1061	10.6	2.2	1.8	4	77200	4			S-
BEAGLE DOG	800H	2221-02	M	77196	1140	9.1	2.1	1.8					1811	LTR
BEAGLE DOG	912A	2221-03	M	77196	762	12.4	2.3	1.6	1462	81197	1462			S-
BEAGLE DOG	841U	2222-01	F	77200	1061	6.1	2.2	1.8	547	79017	547			S-
BEAGLE DOG	792B	2222-02	M	77200	1168	13.0	2.2	1.8	547	79017	547			S-
BEAGLE DOG	901T	2222-03	F	77200	817	10.2	2.0	1.7		80139	1034			D-LTR
BEAGLE DOG	794A	2223-01	M	77201	1163	9.4	2.2	1.8	730	79201	730			S-
BEAGLE DOG	852S	2223-02	F	77201	1017	6.9	2.2	1.8	365	78206	370			S-
BEAGLE DOG	974V	2223-03	F	77201	610	9.3	2.4	1.8					1806	LTR
BEAGLE DOG	695B	2224-01	M	77202	1627	10.6	2.1	1.8	0	77202	0			S-
BEAGLE DOG	857W	2224-02	F	77202	985	10.5	2.3	1.9		80290	1183			D-LTR
BEAGLE DOG	897A	2224-03	M	77202	833	11.4	2.1	1.8	4	77206	4			S-
RHESUS MONKEY	883	2253-01	M	77234	5-7YRS-B	7.2	2.0	1.7	547	79054	550			S-
CYNOMOLGUS MONKEY	37	2253-02	M	77234	3-5YRS-B	3.9	2.1	1.8	1462	81233	1460			S-
CYNOMOLGUS MONKEY	40	2253-03	M	77234	3-5YRS-B	3.8	2.1	1.7	730	79234	730			S-
RHESUS MONKEY	891	2254-01	M	77235	5-7YRS-B	4.3	2.4	1.8	0	77235	0			S-
CYNOMOLGUS MONKEY	33	2254-02	M	77235	2-4YRS-B	2.6	2.2	1.8	64	77299	64			S-
CYNOMOLGUS MONKEY	41	2254-03	M	77235	3-5YRS-B	3.7	2.6	1.9	365	78235	365			S-
CYNOMOLGUS MONKEY	45	2254-04	M	77235	5-7YRS-B	4.1	2.3	1.8					1772	LTR
CYNOMOLGUS MONKEY	30	2255-02	M	77236	3-5YRS-B	3.9	2.2	1.7					1771	LTR
RHESUS MONKEY	874	2265-01	M	77238	5-7YRS-B	4.4	2.0	1.7	4	77242	4			S-
FISCHER-344 RATS		2217-01	M	77195	9WKS		2.2	2.0		79063	598			D-SQU-CELL CARC.LUNG
FISCHER-344 RATS		2217-02	M	77195	9WKS		2.2	2.0	0	77195	0			S-
FISCHER-344 RATS		2217-03	M	77195	9WKS		2.2	2.0	64	77262	67			S-
FISCHER-344 RATS		2217-04	M	77195	9WKS		2.2	2.0		78358	528			D-SQU-CELL PAPILLOMA
FISCHER-344 RATS		2217-05	M	77195	9WKS		2.2	2.0	4	77199	4			S-
FISCHER-344 RATS		2217-06	M	77195	9WKS		2.2	2.0	547	79015	550			S-
FISCHER-344 RATS		2217-07	M	77195	9WKS		2.2	2.0	365	78195	365			S-
FISCHER-344 RATS		2217-08	M	77195	9WKS		2.2	2.0	547	79015	550			S-
FISCHER-344 RATS		2217-09	M	77195	9WKS		2.2	2.0	64	77262	67			S-
FISCHER-344 RATS		2217-10	M	77195	9WKS		2.2	2.0	4	77199	4			S-
FISCHER-344 RATS		2217-11	M	77195	9WKS		2.2	2.0	0	77195	0			S-
FISCHER-344 RATS		2217-12	M	77195	9WKS		2.2	2.0	365	78195	365			S-
FISCHER-344 RATS		2217-13	M	77195	9WKS		2.2	2.0	64	77262	67			S-
FISCHER-344 RATS		2217-14	M	77195	9WKS		2.2	2.0		79165	700			D-SQU-CELL CARC.LUNG
FISCHER-344 RATS		2217-15	M	77195	9WKS		2.2	2.0		78341	511			D-SQU-CELL CARC.LUNG
FISCHER-344 RATS		2217-16	M	77195	9WKS		2.2	2.0		77195	0			D-DURING EXPOSURE
FISCHER-344 RATS		2217-17	M	77195	9WKS		2.2	2.0		79157	692			D-SQU-CELL CA.,ADENO.

B-PRIMATE CAUGHT IN THE WILD, AGE ESTIMATED FROM BODY WEIGHT AT EXPOSURE

D-SPONTANEOUS DEATH

E-EUTHANIZED

S-SACRIFICED

LTR-LONG TERM RESERVE

STATUS OF INHALATION STUDIES OF 850 C HEAT-TREATED PUO2 AEROSOLS FROM THE W-BLENDING OPERATION
AT BABCOCK AND WILCOX IN BEAGLE DOGS, MONKEYS AND FISCHER-344 RATS (CONTINUED)

SPECIES	NUMBER		SEX	DATE	EXPOSURE	WT. (KG)	EXP. AMAD (UM)	AEROSOL SIGMA	PROJ. DEATH SAC. DATE DPE	DPE	ALIVE	COMMENT
	TT00	RADIO			AGE (DAYS)						DPE 6-30-82	
FISCHER-344 RATS		2217-18	M	77195	9WKS		2.2	2.0		79158	693	D-SQU. CELL CARC. LUNG
FISCHER-344 RATS		2217-19	M	77195	9WKS		2.2	2.0	547	79015	550	S-
FISCHER-344 RATS		2217-20	M	77195	9WKS		2.2	2.0		77195	0	D-DURING EXPOSURE
FISCHER-344 RATS		2217-21	F	77195	9WKS		2.2	2.0	365	78195	365	S-
FISCHER-344 RATS		2217-22	F	77195	9WKS		2.2	2.0	547	79015	550	S-
FISCHER-344 RATS		2217-23	F	77195	9WKS		2.2	2.0	730	79197	732	S-
FISCHER-344 RATS		2217-24	F	77195	9WKS		2.2	2.0	64	77262	67	S-
FISCHER-344 RATS		2217-25	F	77195	9WKS		2.2	2.0	0	77195	0	S-
FISCHER-344 RATS		2217-26	F	77195	9WKS		2.2	2.0	64	77262	67	S-
FISCHER-344 RATS		2217-27	F	77195	9WKS		2.2	2.0	365	78195	365	S-
FISCHER-344 RATS		2217-28	F	77195	9WKS		2.2	2.0	4	77199	4	S-
FISCHER-344 RATS		2217-29	F	77195	9WKS		2.2	2.0		78225	395	D-HEMANGIOSARC. LUNG
FISCHER-344 RATS		2217-30	F	77195	9WKS		2.2	2.0		79054	589	D-HEMANGIOSARC. LUNG
FISCHER-344 RATS		2217-31	F	77195	9WKS		2.2	2.0		78352	522	D-HEMANGIOSARC. PLEURA
FISCHER-344 RATS		2217-32	F	77195	9WKS		2.2	2.0	0	77195	0	S-
FISCHER-344 RATS		2217-33	F	77195	9WKS		2.2	2.0	4	77199	4	S-
FISCHER-344 RATS		2217-34	F	77195	9WKS		2.2	2.0	730	79197	732	S-
FISCHER-344 RATS		2217-35	F	77195	9WKS		2.2	2.0	730	79197	732	S-
FISCHER-344 RATS		2217-36	F	77195	9WKS		2.2	2.0	547	79015	550	S-
FISCHER-344 RATS		2217-37	F	77195	9WKS		2.2	2.0	365	78195	365	S-
FISCHER-344 RATS		2217-38	F	77195	9WKS		2.2	2.0	730	79197	732	S-
FISCHER-344 RATS		2217-39	F	77195	9WKS		2.2	2.0		79062	597	D-SQU. CELL CARC. LUNG
FISCHER-344 RATS		2217-40	F	77195	9WKS		2.2	2.0	4	79199	4	S-
FISCHER-344 RATS		2217-46	F	77195	9WKS		2.2	2.0	0	77195	0	S-
FISCHER-344 RATS		2217-49	F	77195	9WKS		2.2	2.0		78234	404	D-FIBROSARC. PLEURA

B-PRIMATE CAUGHT IN THE WILD, AGE ESTIMATED FROM BODY WEIGHT AT EXPOSURE

D-SPONTANEOUS DEATH

E-EUTHANIZED

S-SACRIFICED

LTR-LONG TERM RESERVE

STATUS OF INHALATION STUDIES OF 850 C HEAT-TREATED PUO2, MIXED WITH UO2
AND ORGANIC BINDERS(PELLET PRESSING AT BARCOCK AND WILCOX) IN FISCHER-344 RATS
(PILOT STUDY)

SPECIES	NUMBER		SEX	DATE	EXPOSURE		WT. (KG)	EXP. AEROSOL		PROJ. SAC.	DEATH DATE	DPE	ALIVE DPE 6-30-R2	COMMENT
	TT00	RADIO-			AGE (DAYS)	AGE		AMAD (UM)	SIGMA					
FISCHER-344 RATS		1933-01	M	76348	9WKS			1.7	2.6	0	76348	0		S-
FISCHER-344 RATS		1933-02	M	76348	9WKS			1.7	2.6	0	76348	0		S-
FISCHER-344 RATS		1933-03	M	76348	9WKS			1.7	2.6	0	76348	0		S-
FISCHER-344 RATS		1933-04	F	76348	9WKS			1.7	2.6	0	76348	0		S-
FISCHER-344 RATS		1933-05	F	76348	9WKS			1.7	2.6	0	76348	0		S-
FISCHER-344 RATS		1933-06	F	76348	9WKS			1.7	2.6	8	76356	8		S-
FISCHER-344 RATS		1933-07	F	76348	9WKS			1.7	2.6	8	76356	8		S-
FISCHER-344 RATS		1933-08	F	76348	9WKS			1.7	2.6	8	76356	8		S-
FISCHER-344 RATS		1933-09	F	76348	9WKS			1.7	2.6	8	76356	8		S-
FISCHER-344 RATS		1933-10	F	76348	9WKS			1.7	2.6	8	76356	8		S-
FISCHER-344 RATS		1933-11	M	76348	9WKS			1.7	2.6	16	76364	16		S-
FISCHER-344 RATS		1933-12	M	76348	9WKS			1.7	2.6	16	76364	16		S-
FISCHER-344 RATS		1933-13	F	76348	9WKS			1.7	2.6	16	76364	16		S-
FISCHER-344 RATS		1933-14	F	76348	9WKS			1.7	2.6	16	76364	16		S-
FISCHER-344 RATS		1933-15	F	76348	9WKS			1.7	2.6	16	76364	16		S-
FISCHER-344 RATS		1933-16	M	76348	9WKS			1.7	2.6	64	77046	64		S-
FISCHER-344 RATS		1933-17	F	76348	9WKS			1.7	2.6	64	77046	64		S-
FISCHER-344 RATS		1933-18	F	76348	9WKS			1.7	2.6	64	77046	64		S-
FISCHER-344 RATS		1933-19	F	76348	9WKS			1.7	2.6	32	77014	32		S-
FISCHER-344 RATS		1933-20	F	76348	9WKS			1.7	2.6		78108	491		D-SQU.CELL CA.,PAPIL.LUNG
FISCHER-344 RATS		1933-21	F	76348	9WKS			1.7	2.6		78070	453		D-SQU.CELL PAPILLOMA
FISCHER-344 RATS		1933-22	M	76348	9WKS			1.7	2.6	64	77046	64		S-
FISCHER-344 RATS		1933-23	M	76348	9WKS			1.7	2.6		79071	819		E-ADENOCARC.LUNG
FISCHER-344 RATS		1933-24	M	76348	9WKS			1.7	2.6	32	77014	32		S-
FISCHER-344 RATS		1933-25	M	76348	9WKS			1.7	2.6		78253	636		D-SQU.CELL CARC.
FISCHER-344 RATS		1933-26	M	76348	9WKS			1.7	2.6	32	77014	32		S-
FISCHER-344 RATS		1933-27	M	76348	9WKS			1.7	2.6	64	77046	64		S-
FISCHER-344 RATS		1933-28	M	76348	9WKS			1.7	2.6	32	77014	32		S-
FISCHER-344 RATS		1933-29	M	76348	9WKS			1.7	2.6		77351	369		D-LARGE LUNG MASS
FISCHER-344 RATS		1933-30	M	76348	9WKS			1.7	2.6	32	77014	32		S-
FISCHER-344 RATS		1933-31	M	76348	9WKS			1.7	2.6		77192	210		D-ADENOCARC.LUNG
FISCHER-344 RATS		1933-32	F	76348	9WKS			1.7	2.6		78118	501		D-SQU.CELL CARC.LUNG

D-SPONTANEOUS DEATH
S-SACRIFICED
E-EUTHANIZED

NRC FORM 335 (7-77)		U.S. NUCLEAR REGULATORY COMMISSION BIBLIOGRAPHIC DATA SHEET		1. REPORT NUMBER (Assigned by DDC) NUREG/CR-3313 LMF-105	
4. TITLE AND SUBTITLE (Add Volume No., if appropriate) Radiation Dose Estimates and Hazard Evaluations for Airborne Radionuclides Annual Progress Report July 1, 1981-June 30, 1982				2. (Leave blank)	
7. AUTHOR(S) J. A. Mewhinney				3. RECIPIENT'S ACCESSION NO.	
9. PERFORMING ORGANIZATION NAME AND MAILING ADDRESS (Include Zip Code) Inhalation Toxicology Research Institute Lovelace Biomedical & Environmental Research Institute P. O. Box 5890 Albuquerque, New Mexico 87185				5. DATE REPORT COMPLETED MONTH YEAR February 1983	
12. SPONSORING ORGANIZATION NAME AND MAILING ADDRESS (Include Zip Code) Division of Health, Siting and Waste Management Office of Nuclear Regulatory Research U.S. Nuclear Regulatory Commission Washington, DC 20555				DATE REPORT ISSUED MONTH YEAR June 1983	
13. TYPE OF REPORT Technical				6. (Leave blank)	
15. SUPPLEMENTARY NOTES				8. (Leave blank)	
16. ABSTRACT (200 words or less) The objective of this project is to conduct confirmatory research on aerosol characteristics and the resulting radiation dose distribution in animals following inhalation and to provide prediction of health consequences in humans due to airborne radioactivity which might be released in normal operations or under accident conditions during production of nuclear fuel composed of mixed oxides of U and Pu. Four research reports summarize the results of specific areas of research. The first paper details development of a method for determination of specific surface area of small samples of mixed oxide or pure PuO ₂ particles. The second paper details the extension of the biomathematical model previously used to describe retention, distribution and excretion of Pu from these mixed oxide aerosols to include a description of Am and U components of these aerosols. The third paper summarizes the biological responses observed in radiation dose pattern studies in which dogs, monkeys and rats received inhalation exposures to either 750°C heat treated UO ₂ + PuO ₂ , 1750°C heat-treated (U,Pu)O ₂ or 850°C heat-treated "pure" PuO ₂ . The fourth paper described dose-response studies in which rats were exposed to (U,Pu)O ₂ or "pure" PuO ₂ . This paper updates earlier reports and summarizes the status of animals through approximately 650 days after inhalation.				10. PROJECT/TASK/WORK UNIT NO.	
17. KEY WORDS AND DOCUMENT ANALYSIS Mixed oxide, aerosol, airborne radioactivity, inhalation, exposure, dose, solubility, biological effects, health consequences, risk estimates				11. CONTRACT NO. FIN A1031	
17a. DESCRIPTORS rats Beagles uranium plutonium				14. (Leave blank)	
17b. IDENTIFIERS/OPEN-ENDED TERMS				19. SECURITY CLASS (This report) Unclassified	
18. AVAILABILITY STATEMENT Unlimited				20. SECURITY CLASS (This page) S	
21. NO. OF PAGES				22. PRICE	

UNITED STATES
NUCLEAR REGULATORY COMMISSION
WASHINGTON, D.C. 20555

OFFICIAL BUSINESS
PENALTY FOR PRIVATE USE, \$300

FOURTH CLASS MAIL
POSTAGE & FEES PAID
USNRC
WASH D C
PERMIT NO. 662

120555078877 1 1ANIRH
US NRC
ADM-DIV OF TIDC
POLICY & PUB MGT BR-PDR NUREG
W-501
WASHINGTON
DC 20555

NUREG/CR-3313
RADIATION DOSE ESTIMATES AND HAZARD EVALUATIONS
FOR INHALED AIRBORNE RADIOISOTOPES

JUNE 1983